SPATIAL ANALYSIS OF WARM SEASON URBAN LIGHTNING ENHANCEMENT IN THE CHARLANTA MEGAREGION

by

JEFFERY DANIEL BURKE

(Under the Direction of J. Marshall Shepherd)

ABSTRACT

Within the Charlotte, North Carolina, to Atlanta, Georgia, megaregion (Charlanta), the Atlanta metropolitan area has been shown to augment proximal cloud-to-ground (CG) lightning occurrence through a variety of hypothesized mechanisms. Although numerous studies have investigated this urban lightning effect (ULE), there is currently a knowledge gap regarding patterns of urban flash enhancement at the scale of the entire Charlanta megaregion. Moreover, no urban lightning study to date has analyzed total lightning (TL) observations from the Geostationary Lightning Mapper (GLM) aboard GOES-16. Filling these areas of need, a novel climatological synthesis of urban CG and TL flash modification across Charlanta was constructed using data collected by the U.S. National Lightning Detection Network and the GLM. Specifically, this research investigated spatial distributions of CG and TL around Atlanta, GA, Greenville, SC, and Charlotte, NC, during the warm seasons of 2007–2021. Augmentation of lightning intensity and frequency was apparent over and downwind of the larger cities in both forms of detection data, with a diminished urban signal over the smaller city of Greenville.

INDEX WORDS: Urban lightning, Charlanta megaregion, Geostationary Lightning Mapper

SPATIAL ANALYSIS OF WARM SEASON URBAN LIGHTNING ENHANCEMENT IN THE CHARLANTA MEGAREGION

by

JEFFERY DANIEL BURKE

B.S., University of Georgia, 2020

A Thesis Submitted to the Graduate Faculty of The University of Georgia in Partial Fulfillment of the Requirements for the Degree

MASTER OF SCIENCE

ATHENS, GEORGIA

2022

SPATIAL ANALYSIS OF WARM SEASON URBAN LIGHTNING ENHANCEMENT IN THE CHARLANTA MEGAREGION

by

JEFFERY DANIEL BURKE

Major Professor:	Marshall Shepherd
Committee:	John Knox
	Tom Mote

Electronic Version Approved:

Ron Walcott
Vice Provost for Graduate Education and Dean of the Graduate School
The University of Georgia
December 2022

ACKNOWLEDGEMENTS

First and foremost, I want to thank my major professor, Dr. Marshall Shepherd, for his invaluable guidance, patience, and encouragement throughout the completion of this thesis, and most importantly, for the opportunity to complete my graduate education at the University of Georgia. I also want to thank fellow committee members, Dr. John Knox and Dr. Tom Mote, for their advice and support. During my time as an undergraduate student, Dr. Knox provided me with the inspiration and confidence to pursue graduate research, while Dr. Mote's challenging course instruction instilled a sense of attention to detail that has been integral to my success. I would also like to acknowledge support from the NASA Interdisciplinary Research in Earth Science program (80NSSC20K1268). Lastly, I want to express sincere gratitude to my girlfriend, Emily Johnson, for her daily sacrifices and unwavering support throughout this process.

TABLE OF CONTENTS

Page

LIST OF TABLES

Page

LIST OF FIGURES

Page

CHAPTER 1

INTRODUCTION

The Atlanta metropolitan area has been the focus of numerous investigations into urban influences on local atmospheric conditions and their signal in climatological trends (Debbage & Shepherd, 2018; McLeod and Shepherd, 2022; McLeod et al., 2017; Shepherd et al., 2014, 2015). A constituent of the larger Piedmont Ecoregion, the Charlanta megaregion contains the Atlanta, Greenville-Spartanburg, and Charlotte Metropolitan Statistical Areas (MSAs) as displayed in Figure 1.1. Charlanta consists of a rapidly developing Urban Climate Archipelago (UCA) roughly following Interstate-85 between Atlanta, GA, and Charlotte, NC. Shepherd et al. (2014) defined a UCA as a chain or aggregate of urban areas that modify aspects of the climate system. Increasing contiguity of impervious surfaces and expansion of urban sprawl along the periphery are predicted to dramatically alter the spatial footprints of individual cities and the structure of the entire Charlanta UCA in the coming years, emphasizing the need for continued research on land-atmosphere interactions at the scale of the megaregion (Stone et al., 2013; Terando et al., 2014).

The "urban lightning effect" (ULE) describes the observed tendency of large urban areas to augment proximal flash production through a variety of mechanisms (Shepherd et al., 2015; Stallins and Rose, 2008). This phenomenon has been thoroughly investigated over the years, producing the consensus that major cities generally serve as positive forcings for thunderstorms and the lightning strikes they manifest. More specifically, major cities display a propensity to significantly modify the spatio-temporal characteristics of lightning associated with weakly-

forced thunderstorms (WFTs; Ashley et al., 2012; Rose et al., 2008; Stallins and Rose, 2008). With atmospheric conditions supportive of WFTs in the eastern US expected to become more prevalent in the future (Diffenbaugh et al., 2013; Miller and Mote, 2017b), it can be inferred that so too will the occurrence of lightning. Furthermore, the rapid development of urban centers and megaregions such as Charlanta will alter the local forcings driving the ULE. These conditions underlie the need for continued investigation and monitoring of urban influences on lightning production.

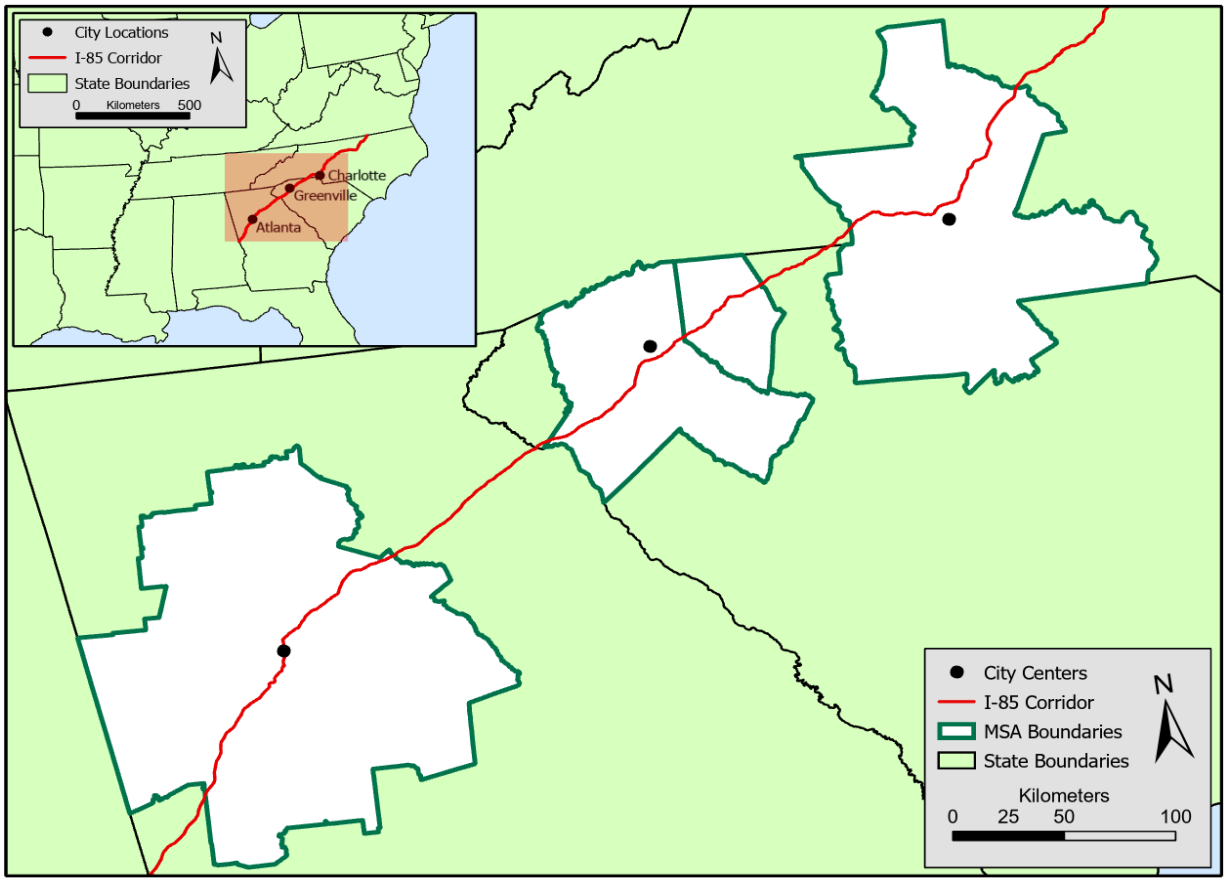

Figure 1.1: Location of the Charlanta I-85 corridor and the MSAs of Atlanta, GA, Greenville, SC, and Charlotte, NC.

While the last two decades have produced numerous inquiries into anthropogenic forcings on local meteorological and hydrological variables (e.g., temperature, precipitation) across major cities throughout the Southeast (Debbage and Shepherd, 2018; Diem and Mote, 2005; Shepherd, 2005; Shepherd et al., 2011; McLeod et al., 2017; Mote et al., 2007), there exists a roughly 15-year (2007–2021) knowledge gap regarding spatial distributions of urban CG lightning modification that is yet to be filled. Ashley et al. (2012) and Stallins et al. (2012) analyzed CG flash distributions during 1997–2006 and 1995–2008, respectively, representing the most recent assessments of the ULE in the Southeast. Moreover, although the urban corridor of the Charlanta megaregion has recently become the focus of significant research, there has yet to be an investigation of the ULE at the spatial scale of the entire megaregion. Notwithstanding that many urban lightning studies have analyzed flash observations from ground-based networks of detection antennae, comparatively few have utilized observations from spaceborne sources. Additionally, few studies of the ULE have analyzed aggregated IC, CG, and CC flash observations, collectively referred to as "total lightning" (TL). The novel availability of high-resolution TL data collected by the spaceborne Geostationary Lightning Mapper (GLM) presents contemporary researchers of the ULE with a convenient source for reliable TL observations.

To fill the aforementioned knowledge gap in urban lightning research, this thesis pursued the following questions (Q1 & Q2) and accompanying hypotheses (H1 & H2):

Q1: How do spatial distributions of warm season lightning derived from an extended record of observation within the Charlanta megaregion compare to patterns identified by previous work focused on individual cities?

H1: The well-documented spatial patterns of the warm season ULE are strongly correlated with city-scale characteristics (e.g., size, density, layout, etc.) that are in a continuous state of

rapid change, most prominently in the form of outward growth and densification. Thus, it is hypothesized that these patterns of proximal lightning enhancement associated with major cities will display an attendant spatio-temporal evolution that is observable at the megaregion-scale.

Q2: Is urban lightning enhancement in Charlanta resolvable in TL data collected by the GLM aboard GOES-16?

H2: Major cities have displayed a propensity to augment convective intensity, most vigorously that of WFTs. As it is well established that TL serves as a robust proxy for convective intensity due to the overwhelming predominance of IC flashes relative to CG strikes (MacGorman et al., 2011), it is hypothesized that the characteristic patterns of the ULE will be clearly observed in the first four years (2018–2021) of TL data from the GLM.

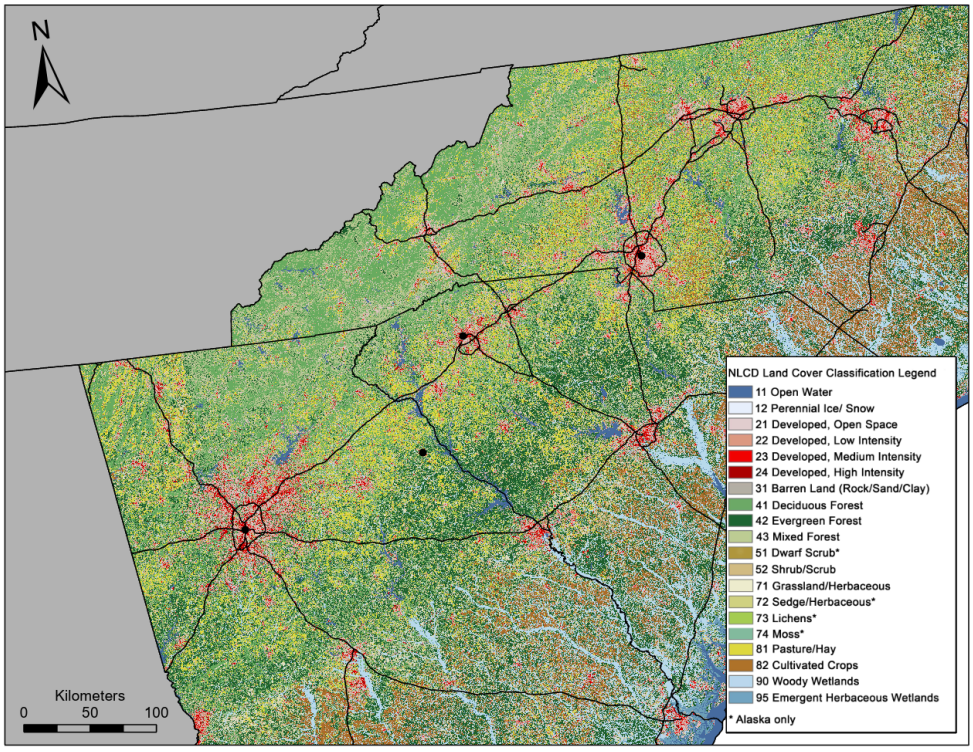

Figure 1.2: 2011 National Land Cover Database (NLCD) land cover classification of the Charlanta megaregion.

Following this introductory section, the structure of the thesis is divided into four chapters. Chapter two covers relevant background information: the principles of cloud electrification, lightning detection from space, and the patterns and mechanisms of the ULE. Chapter three describes the details of the research design, including the utilized datasets and methods of analysis. Chapter four discusses the results of the implemented design, and finally, chapter five synthesizes the conclusions of the work.

CHAPTER 2

LITERATURE REVIEW

As noted by Stallins and Rose (2008), previous studies of urban lightning can be broadly grouped into two modes of inquiry: those taking a "descriptive phenomenological approach" and those taking a "foundational approach." Those in the former have sought to explore spatio-temporal distributions of urban lightning through pattern analysis, visualization, and statistical inference, while those in the latter have focused on generating clearer understandings of the physical mechanisms driving the ULE. Therefore, contemporary pursuits must consider these inherent differences when synthesizing past research and formulating their own methodological approach. Additionally, as much of the past research into urban effects has focused on larger-scale results of convection (i.e., precipitation) rather than lightning occurrence, the conclusions of these studies must be considered with that in mind. Nevertheless, as lightning is inherently a manifestation of convective processes, these studies provide valuable context for the effects of urban areas on proximal lightning occurrence (Shepherd et al., 2015).

2.1 Cloud electrification and discharge

Although an understanding of the basic microphysical processes leading to lightning initiation is well developed, the specific details that explain the generation of the main cloud charge dipole are less so (Uman, 2001). Here I provide a brief review of the most widely accepted mechanism of cloud electrification, known as the non-inductive charge separation process (MacGorman and Rust, 1998; Rakov and Uman, 2006; Uman, 2001). Within the mixed

phase region of a cumulonimbus cloud, collisions between ascending supercooled water droplets and ice crystals with descending graupel leads to the transfer and accumulation of positive and negative charges. The influence of gravity and updrafts results in the separation of opposite charges, as heavier, negatively charged particles fall toward the surface while lighter, positively charged particles rise to the upper portion of the cloud. After a breakdown of voltage potential, a channel of ionized air is generated through which an initial flow of electrons, known as a leader, acts to equalize the differences in charge (Uman, 2001). These processes constitute our current understanding of lightning initiation.

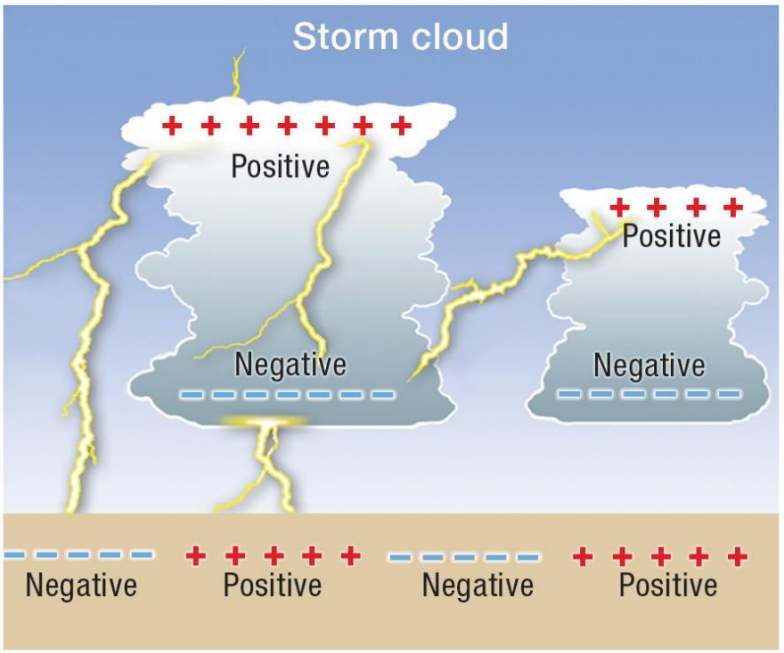

Figure 2.1: Elementary illustration of a thunderstorm's electrical charge structure and associated forms of lightning discharge (*A Bolt from the Blue*, 2019).

As depicted in Figure 2.1 above, there are three main forms of lightning discharge categorized by their spatial characteristics: cloud-to-ground (CG), intra-cloud (IC), and cloud-to-cloud (CC). CC discharges are relatively rare and as a result, they often go unmentioned. IC lightning flashes make up the vast majority of discharges globally, with CG strikes representing

a small fraction (Uman, 2001). Between both forms of lightning, Medici et al. (2017) reported an IC:CG ratio of ~2–3 throughout the Charlanta megaregion. Lightning strikes can be further grouped into positive and negative polarity flashes, although positive flashes are relatively rare, representing just 4% of total flashes on average (Orville et al., 1983; Uman, 2001). Since 1989, Vaisala's US National Lightning Detection Network (NLDN) has collected spatially explicit lightning data via an array of ground-based sensors with recent network upgrades achieving detection efficiencies upwards of 93% for CG flashes (Murphy et al., 2021). This network, along with its spaceborne counterparts, has paved the way for much of the ground-breaking lightning research that has occurred over the last three decades.

2.2 Lightning phenomenology

2.2.1 Lightning detection from space

While global networks detecting total lightning flashes have been widely operated for many years, regional and continental CG detection networks such as the NLDN have been the preferred sources of flash data for analyses of urban-related lightning enhancement (Cummins and Murphy, 2009). This is largely due to a number of undesirable characteristics associated with detection of lightning flashes at a global scale, namely, low detection efficiencies and spatio-temporal variations in accuracy (Bürgesser, 2017; Hayward et al., 2020; Lay et al., 2005). The now defunct spaceborne Lightning Imaging Sensor (LIS) and its antecedent prototype aboard *MicroLab-1*, known as the Optical Transient Detector (OTD), suffered from similar data accuracy and consistency issues due to the low earth orbit (LEO) of the Tropical Rainfall Measuring Mission (TRMM) satellite, which resulted in discontinuous spatio-temporal coverage and middling detection efficiencies (Boccippio et al., 2000, 2002; Hayward et al., 2020;

Thompson et al., 2014). To remedy the known pitfalls of lightning detection via satellites in LEO, NASA and NOAA jointly launched the GLM aboard the Geostationary Operational Environmental Satellite (GOES) R-series in 2016, marking the advent of spatially and temporally continuous lightning detection from space (Goodman et al., 2013; Medici et al., 2017).

As detailed by Rudlosky et al. (2019), the GLM instrument consists of a charge-coupled device (CCD) imager that detects near-infrared (NIR) emissions within a narrow 1 nm band centered at 777.4 nm. The GLM's CCD provides an at-nadir spatial resolution of 8 km and a field-of-view encompassing much of the western hemisphere (+/- 54° in latitude). In principle, the GLM observes the momentary changes in an optical scene associated with the NIR cloud top emissions produced by lightning. Following at-sensor collection, the raw observations are transmitted to the GOES ground-processing system which filters out non-lightning events and clusters the remaining lightning events into groups and flashes through the Lightning Cluster Filter Algorithm (LCFA; Goodman et al., 2013; Rudlosky et al., 2019). After downstream processing, the final GLM products have a daytime (nighttime) flash detection efficiency (DE) greater than 70% (90%) and location accuracy of approximately 4 km (Koshak et al., 2018; Rudlosky et al., 2019). Though the data produced by the GLM and its accompanying LCFA are most prominently used to enhance the short-term forecasting abilities of the National Weather Service (NWS), a primary objective of the sensor is to provide spatio-temporally continuous lightning observations for use in long-term climatological analyses (Rudlosky et al. 2019; Rudlosky et al. 2020). Moreover, Rudlosky et al. (2020) note that TL properties are best observed from space, further supporting its use in studies of urban influences on TL production.

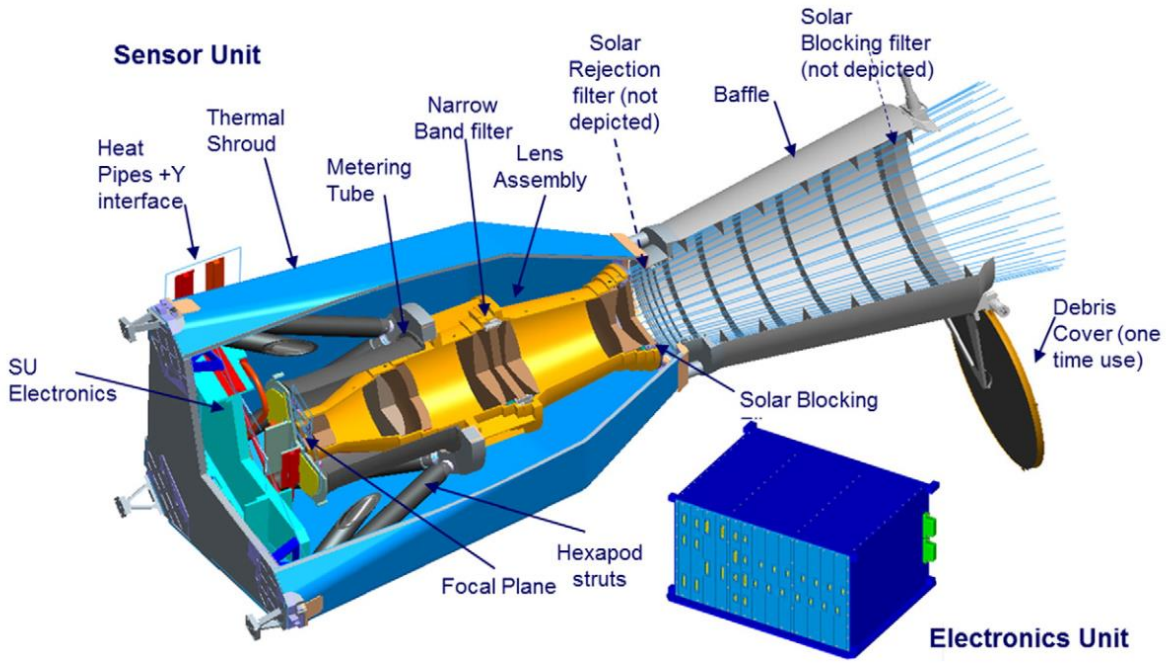

Figure 2.2: The sensor and electronics units of the GLM (Goodman et al., 2013).

2.2.2 Patterns of the ULE identified in past work

As one of the first studies to utilize CG flash data collected by the NLDN, Westcott (1995) analyzed the frequency of summertime lightning flashes immediately upwind and downwind of 16 central US cities over a period of four years (1989–1992), reporting an enhancement of 40%–85% in negative CG flash densities over and downwind of the urban centers. Several studies conducted by the Houston Environmental Aerosol Thunderstorm (HEAT) project found a 20% decrease and 58% increase in positive and negative summertime flash densities, respectively, over and downwind of the Houston metro area (Orville et al., 2001; Steiger et al., 2002; Steiger and Orville, 2003). Additionally, they found a 7% increase in lightning days over Houston, or the days in which at least one lighting strike was detected (Steiger et al., 2002). More recently, Kingfield et al. (2018) conducted a comparative analysis of thunderstorm frequency in and around 4 urban areas of the central US (Dallas-Fort Worth, TX; Minneapolis-St. Paul, MN; Oklahoma City, OK and Omaha, NE). Their results displayed a

24%–50% increase in the number of downwind thunderstorms during days with weak synoptic forcing.

Focusing on the Atlanta metropolitan area, numerous studies have investigated the spatio-temporal patterns of urban effects on convective processes (Diem, 2008; Diem and Mote, 2005; Dixon and Mote, 2003; Haberlie et al., 2016; McLeod and Shepherd, 2022; McLeod et al., 2017; Mote et al., 2007; Rose et al., 2008; Shepherd et al., 2002, 2015; Stallins and Bentley, 2006; Stallins et al. 2006; Stallins and Rose, 2008; Watson and Holle, 1996). Most notably in the area of urban lightning research, Stallins et al. (2006) found that average annual CG flash densities in Atlanta during 1992–2003 were 50%–75% higher than in surrounding rural areas. Stallins and Bentley (2006) documented the dependence of spatial patterns on synoptic conditions, with flash densities and flash days under synoptically benign conditions tending to cluster tightly within the developed center and urban corridors of Atlanta (displayed in Figure 3 below). In contrast, they found that synoptically active conditions produced relatively lower values for each flash metric over the city center and a more diffuse spatial distribution overall. Stallins and Rose (2008) constructed a comprehensive summary of urban lightning research to date, including detailed descriptions of approaches, methodologies, and recommendations for future research. Building from the directions for future work suggested by Stallins and Rose (2008), Rose et al. (2008) performed an integrated analysis of warm season lightning and precipitation for the Atlanta metro area. They observed a clear relationship between anomalies of precipitation, lightning, and the prevailing wind direction, affirming the spatial consistency of precipitation and lightning documented in coincident studies (Mote et al., 2007; Stallins and Rose., 2008). Additionally, they verified the importance of synoptically benign conditions in regulating patterns of urban flash enhancement as observed in Stallins and Bentley (2006).

As described by Shepherd et al. (2015), the "urban rainfall effect" (URE) has displayed clear spatio-temporal connections to the ULE. In an integrated study of radar reflectivity and lightning data focused on the Atlanta metro area, Ashley et al. (2012) found statistically significant increases in aggregate (1997–2006) warm season (June-August) CG flash counts and flash days between defined urban-rural boundaries of 34%–42% and 14%–20%, respectively. These increases were accompanied by statistically significant increases in medium and high reflectivity days, further elucidating the spatio-temporal connections between precipitation and lightning. Another key finding of their study was the linkage between patterns of lightning, precipitation, and the geometry of the urban footprint. Finally, McLeod et al. (2017) performed the first climatological analysis of the URE around Atlanta, GA. They reaffirmed the findings of previous analyses, notably, the dependence of urban-influenced downwind precipitation anomalies on the prevailing wind direction. As a result, McLeod et al. (2017) also formally proposed the term "flow regime dependent" to describe the downwind anomaly regions associated with the URE.

In general, the results of these studies display two persistent patterns: (i) the enhancement of CG flash densities and precipitation over and downwind of urban centers and (ii) the suppression of positive polarity CG flashes in proximity to cities. The mechanisms hypothesized to be driving these spatio-temporal patterns will be discussed in the following section (2.3).

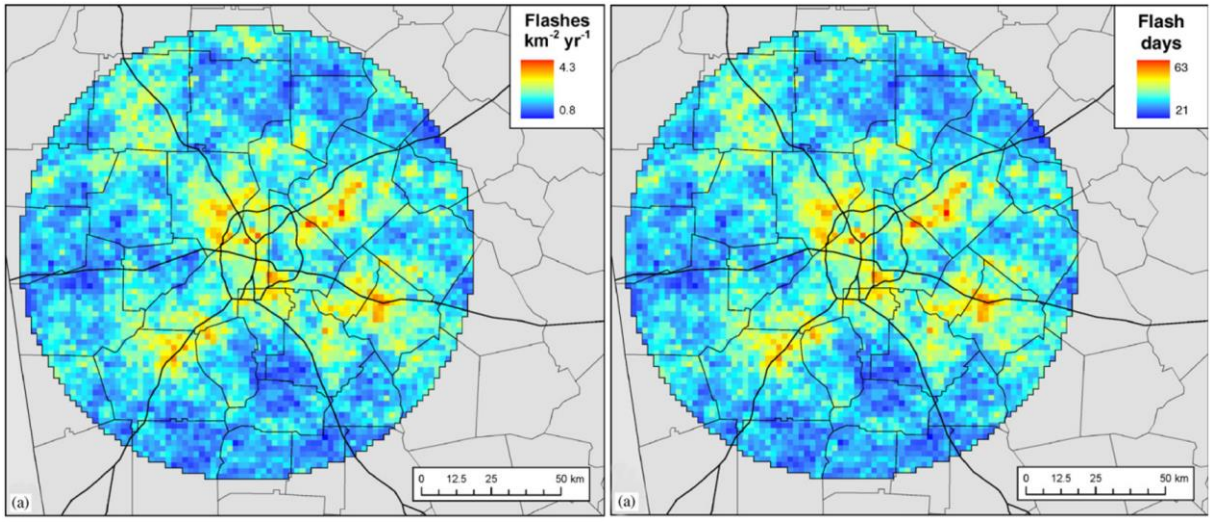

Figure 2.3: CG flash density and days (2 km bins) during synoptically quiescent periods around the Atlanta metropolitan area for the years 1992–2003 from Stallins and Bentley (2006).

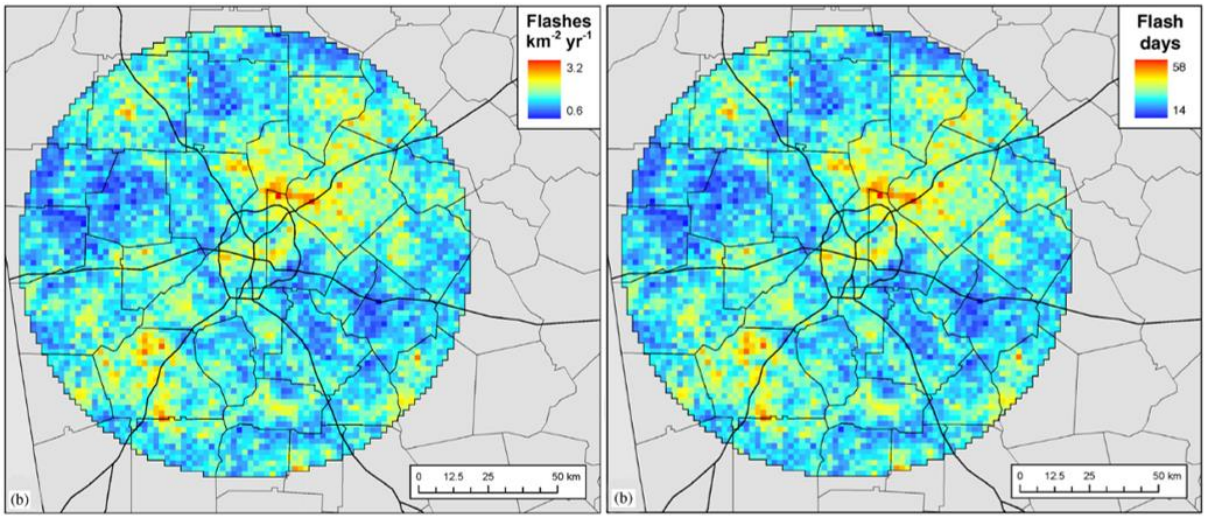

Figure 2.4: CG flash density and days (2 km bins) during synoptically active periods around the Atlanta metropolitan area for the years 1992–2003 from Stallins and Bentley (2006).

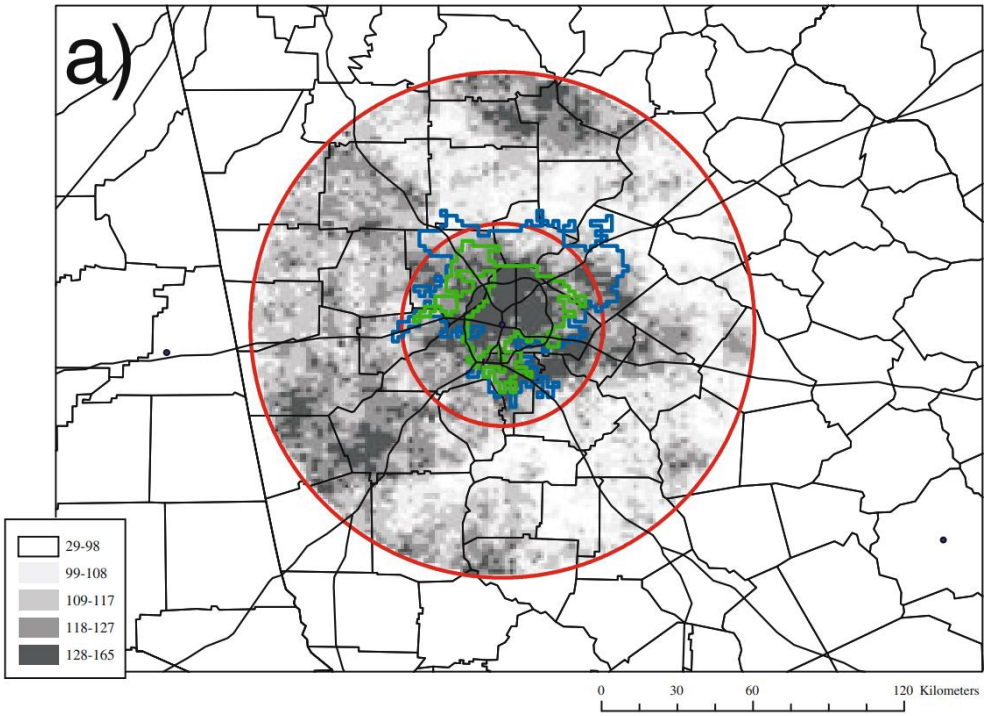

Figure 2.5: Total days with reflectivity ≥ 40 dBZ in each 2 km grid cell for Atlanta, GA between the years 1997–2006. Red circles correspond to urban-rural buffers, while the blue (green) boundaries represent urban delineations derived from NLCD land cover (USGS built-up area) data. As displayed in Ashley et al. (2012).

2.3 Hypothesized mechanisms of urban convective enhancement

Though there are a number of tenable hypotheses explaining the ULE, the complex nature of the multi-scale causal mechanisms underlying the phenomenon has precluded a complete understanding. As described by Stallins and Rose (2008), anthropogenic influences on CG flash production can be broadly grouped into two inter-connected categories: (i) enhancement of local surface convergence and convective instability arising from the characteristics of the urban boundary layer heat island (BLHI) and surface morphology and (ii) modification of the microphysical conditions driving cloud electrification by anthropogenic aerosols. More generally, these can be summarized as thermodynamic, morphological, and microphysical "urban effects." As noted by Shepherd et al. (2015), while the source literature has

well validated the mechanisms by which urban effects modify the frequency and intensity of precipitation, this is not the case for lightning. Nevertheless, the spatio-temporal coincidence between patterns of the URE and ULE makes these conclusions relevant for studies focused on explanations of the latter.

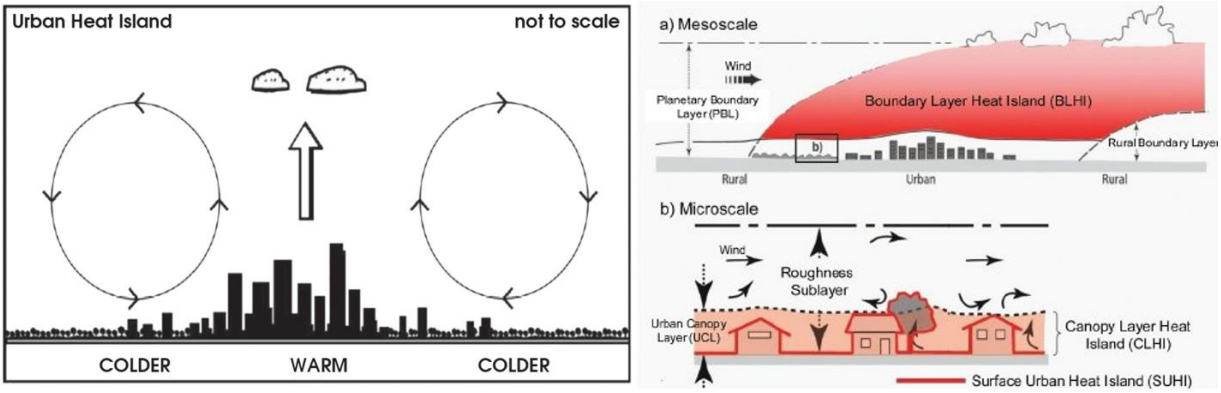

Figure 2.6: Conceptual diagram of UHI-induced meso-circulations (left) from Simpson (2006) and a depiction of the urban boundary layer atmosphere (right) from Srivanit and Hokao (2012).

2.3.1 Thermodynamic effects

The urban heat island (UHI) has long been studied for its role in the modification of local and regional weather and climate (Oke, 1982, 1988; Oke and Cleugh, 1987). Due to the radiative (e.g., albedo, emissivity) and thermal (e.g., heat capacity, thermal conductivity) properties of built-up surfaces, urban areas experience warmer skin, air, and canopy temperatures, giving rise to the BLHI and canopy layer heat island (Heisler and Brazel, 2010; Oke, 1982, 1988; Oke and Cleugh, 1987; Shepherd et al., 2015; CLHI). Numerous modeling experiments have investigated the BLHI, documenting the existence of persistent mesocirculations arising from gradients of both temperature and pressure between urban areas and their rural surroundings (Craig and Bornstein, 2002; Rozoff et al., 2003). As described by Shepherd et al. (2015) and depicted in Figure 2.6, the conceptual arrangement of these urban mesocirculations is akin to the well-known sea-breeze circulation. The dominant result of this arrangement, as documented in a

number of past studies (Baik et al., 2007; Han and Baik, 2007), is a UHI-induced increase in surface convergence and convection downwind of urban centers.

2.3.2 Microphysical effects

The observed increase in aerosol concentrations within the urban boundary layer has long been investigated as a potential forcing for the ULE and URE. Acting as cloud condensation nuclei (CCN), anthropogenic aerosols indirectly influence the formation of precipitation and consequently, the occurrence of lightning (Shepherd, 2005; Shepherd et al., 2015). As noted by Stallins and Rose (2008), relevant studies have found a varying relationship between urban aerosol concentrations and lightning occurrence (Kar et al., 2007; Naccarato et al., 2003; Stallins et al., 2006; Stallins et al., 2012; Steiger and Orville, 2003; Van Den Heever and Cotton, 2007; Westcott, 1995). Stallins et al. (2006) found a spatial correspondence between reduced positive flash occurrence, a commonly identified feature of the ULE, and areas associated with higher aerosol concentration in Atlanta, GA. Van Den Heever and Cotton (2007) displayed the significance of aerosol size and concentration in the timing and location of convection. Using a variety of multivariate techniques to investigate weekly aerosol concentrations in relation to CG lightning occurrence around Atlanta, GA, Stallins et al. (2012) discovered a few notable spatio-temporal patterns. Broadly, their analysis indicated a greater incidence of CG lightning within 100 km of the city center under elevated weekday aerosol concentrations. More specifically, the density of CG lightning flashes was shown to contract towards the city center on weekends, with the most significant weekend-weekday contrast in flash density occurring over non-urban land uses near the perimeter of the Atlanta metro area. The results of these studies outline the hypothesized role of anthropogenic aerosols in the ULE.

CHAPTER 3

RESEARCH DESIGN

Broadly, the purpose of this thesis was to provide a contemporary assessment of the ULE around three major cities in the Southeast US. More specifically, this thesis aimed to fill the roughly 15-year (2007–2021) knowledge gap regarding spatial distributions of CG lightning at the scale of the Charlanta megaregion and to determine if the ULE is resolvable in the first four years (2018–2021) of TL observations from the GLM. The availability of high-resolution TL data collected by the spaceborne GLM presents contemporary researchers of the ULE with a novel source of TL observations yet to be utilized. Furthermore, as it is well established that TL serves as a more robust proxy for convective intensity due to the overwhelming predominance of IC flashes relative to CG strikes (MacGorman et al., 1989; MacGorman et al., 2011), TL observations from the GLM may provide a more complete perspective of urban influences.

During the construction of the workflow detailed in the following sections, relevant methodological recommendations from Lowry (1998), Shepherd (2005), and Shepherd et al. (2015) were strongly considered. In summary, they emphasized the importance of replicating experiments across several urban areas, using control domains, and testing explicitly stated hypotheses with standard statistical methods, among other important features. As a result, and in pursuit of the predefined research questions and hypotheses, 15-year (4-year) warm season aggregate CG (total) lightning climatologies were constructed for the major urban areas of Atlanta, GA, Greenville, SC, Charlotte, NC, and for the entire Charlanta megaregion. Alongside the three urban domains, the predominantly rural city of Elberton, GA was utilized as a control

region. Roughly following the methodology of Ashley et al. (2012), visual and quantitative analyses were performed to develop an intensive climatological synthesis of the contemporary ULE across Charlanta.

3.1 Data

3.1.1 Cloud-to-ground lightning observations

The commercial nature of Vaisala's NLDN results in generally limited public access to its collected and processed observations. Currently, the only public NLDN data is a pared-down product made available through the National Centers for Environmental Information (NCEI) Severe Weather Data Inventory (SWDI; Ansari et al., 2009). The SWDI provides access to spatially aggregated (i.e., gridded) NLDN lightning observations in tabular format containing yearly timeseries of daily CG flash counts across the continental US (CONUS) with coordinates corresponding to a 0.1° latitude-longitude grid (approximately 10 km spatial resolution after projection). With emphasis placed on the utilization of publicly available data sources, daily CG flash counts for the years 2007–2021 were downloaded locally as a comma-separated delimited text (i.e., CSV) file. The 15-year period of record was selected to roughly cover the years since prior analysis in the study area (Stallins et al., 2012). As the NLDN CG data are delivered in CSV format, the R statistical programming language served as the most efficient tool for manipulation and processing to prepare the data for further analysis.

Following acquisition, the CSV file containing the daily CG flash counts was imported into R before being temporally filtered to the months of June, July, and August (JJA), representing the peak of the Southeast's diurnally driven convective season. Based on the

suggestions of previous studies (Ashley et al., 2012; Hayward et al., 2020; Stallins and Rose, 2008), a set of three metrics were derived to quantify CG intensity and frequency, including the total CG flash count over the 15-year study period, the total number of active CG flash days (i.e., days where flash count ≥ 1), and the CG flashes per flash day (i.e., flash count / days). As discussed by Miller (2014), the flashes per flash day metric is utilized to compare cells in terms of the average lightning production during active thunderstorm days. An example of the aggregated CG flash count data is displayed in Figure 3.1 below.

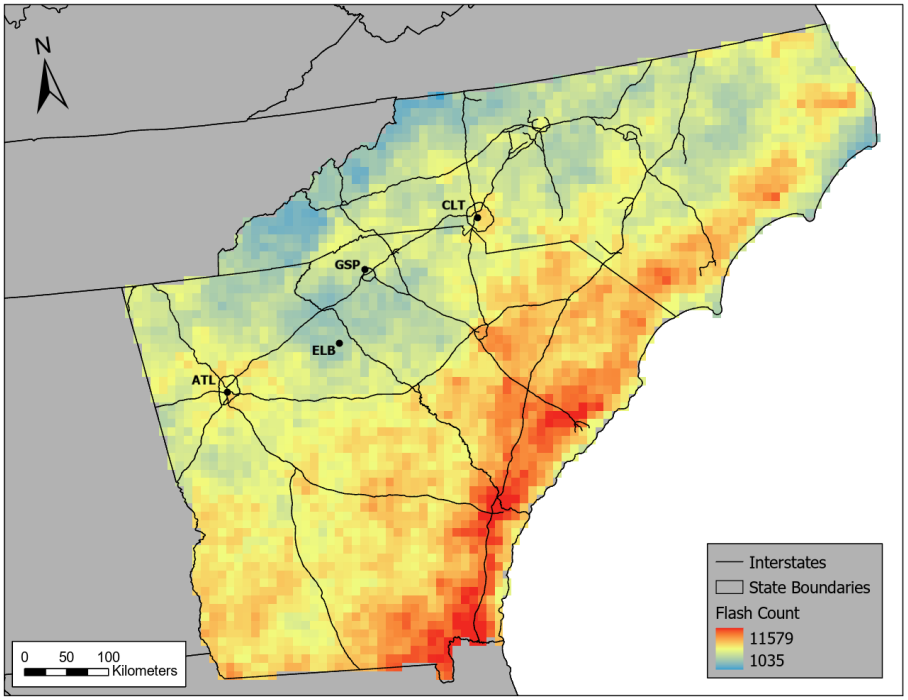

Figure 3.1: Example of aggregated warm season CG flash counts observed by the NLDN for Georgia, South Carolina, and North Carolina over the 15-year study period (2007–2021).

3.1.2 Total lightning observations

Spaceborne TL detection data collected by the GLM is freely available from a number of sources, though not in an optimized format for multi-year analyses. For example, the Amazon Open Data S3 bucket archive of Level 2 (L2) GLM products provides access to the individual

netCDF4 packets containing the lightning events, groups, and flashes produced by the LCFA (Losos et al., 2020). Each packet contains 20 seconds of data at a spatial resolution of approximately 8 km (Koshak et al., 2018). This format is understandable due to the primary utility of GLM data as a short-term forecasting aid but makes for cumbersome processing on longer time scales. The recent work of Oda et al. (2022), which performed a climatological analysis of GLM flash rate density across Brazil, required the procurement of spatially and temporally aggregated GLM observations. In collaboration with the Center for Weather Forecasting and Climate Studies (CPTEC) within Brazil's National Institute for Space Research (INPE) and Dr. Richard Blakeslee of NASA's Marshall Space Flight Center (MSFC), the more than 6 million provisionally mature (i.e., beginning in January of 2018) L2 GLM packets were processed, and the resulting products made publicly-available through a managed file transfer protocol (FTP) archive (CPTEC, 2022; Oda et al., 2022).

As described by Oda et al. (2022), processing by CPTEC accumulated raw 20-second netCDF4 GLM files over 5-minute bins on its at-nadir resolution 8 km x 8 km grid, an optimal format for the requirements of this thesis. Quality control measures were taken by filtering GLM observations to those only with a Data Quality Flag of "good," as recommended by Rudlosky et al. (2019). Though these files include variables derived from all three GLM LCFA classes, the "Group Centroid Density," representing the total number of group centroids detected within each pixel over the 5-minute time interval, is most suitable for a comparative analysis with ground-based CG sources. Consequently, warm season (JJA) TL group observations from the GLM were acquired from CPTEC's public archive in their native netCDF format for a 4-year period (2018–2021), representing the full range of provisionally mature data (Koshak et al., 2018). In order to create the desired TL group climatologies, the Climate Data Operators (CDO; Schulzweida,

2022) suite of command line tools were utilized to further aggregate the data, clip to the desired geographic region, and to derive the desired variables aimed at quantifying TL intensity and frequency: 1) the total group count over the 4-year record of observation, 2) the total number of active TL group days (i.e., days where group count ≥ 1), and 3) the TL groups per group day (i.e., group count / group days).

3.1.3 Physiographic data

Land cover data was acquired from the United States Geological Survey (USGS) National Land Cover Database (NLCD 2011), which provides access to spatially explicit land cover and per-pixel impervious surface products derived from 30 meter Landsat imagery (Dewitz, 2021; Yang et al., 2018). Global Multi-resolution Terrain Elevation Data (GMTED2010; Danielson and Gesch, 2011) from the USGS Earth Resources Observation and Science Center Archive was employed as contextual information to support visual assessment at each scale of analysis. The relatively high spatial resolution (7.5-arc-second) of this topographic information proved useful in identifying lightning hotspots predominantly driven by terrain features.

3.1.3 Wind reanalysis

Recently produced by the European Center for Medium-Range Weather Forecasts (ECMWF), the ERA5 global reanalysis provides gridded (0.25°) hourly wind speed and direction (U and V components) data on 37 pressure levels (1000 hPa to 1 hPa) from 1959 to present, among a number of other atmospheric, oceanic, and land-surface parameters (Hersbach et al. 2020). In order to characterize each city's typical warm season wind regime, the ERA5 U and V wind components for the NLDN CG and GLM TL periods of record (2007–2021 and

2018–2021, respectively) were acquired at the 700 hPa pressure level and processed using the netCDF Operators (NCO) suite of command line programs (Zender, 2022). NCO allowed for efficient calculation of wind speed and direction from the standard U and V components and temporal filtering to the warm season. Similar to McLeod and Shepherd (2022), CDO was utilized to find the average wind speed and direction within the ERA5 reanalysis grid cells roughly covering each city's geometric domain boundary. Finally, the windrose Python library (Roubeyrie and Celles, 2018) was utilized to construct wind rose climatologies for the four city-scale domains. As with the physiographic datasets, these compact depictions of each city's prevailing wind flow conditions during the warm season provided critical support throughout visual analysis of the lightning climatologies.

3.2 Methods

3.2.1 Defining the city-scale domains and Charlanta megaregion

The set of four city-scale domains, consisting of the three cities (Atlanta, Greenville, and Charlotte) and one rural control (Elberton) were constructed in ArcGIS Pro 2.9 using geometric buffers (*ArcGIS Pro*, 2021). The buffers were based around each city's administratively defined center to define the outer boundaries of their domains. Relevant population characteristics and the sizes of the city-scale buffers are displayed in Table 3.1 below. A rectangular polygon feature representing the entire Charlanta megaregion was defined using ArcGIS Pro's *Minimum Bounding Geometry* tool with the three geometric buffers of Charlanta's major cities as the input features. This boundary and its constituent geometric domains are displayed in Figure 3.2 below.

Table 3.1: Population characteristics and buffer sizes of the urban and control domains examined. Domains are ranked by population (U.S. Census Bureau).

City	Population (2010)	Population (2019)	2010–2019 % Change	Urban Buffer Radius (km)	Rural Buffer Radius (km)
Atlanta, GA (ATL)	5,302,598	6,020,364	+13.5%	40	100
Charlotte, NC (CLT)	2,250,121	2,636,883	+17.2%	35	87.5
Greenville, SC (GSP)	1,110,356	1,240,262	+11.7%	30	75
Elberton, GA (ELB)	4,570	4,329	-5.3%	35	87.5

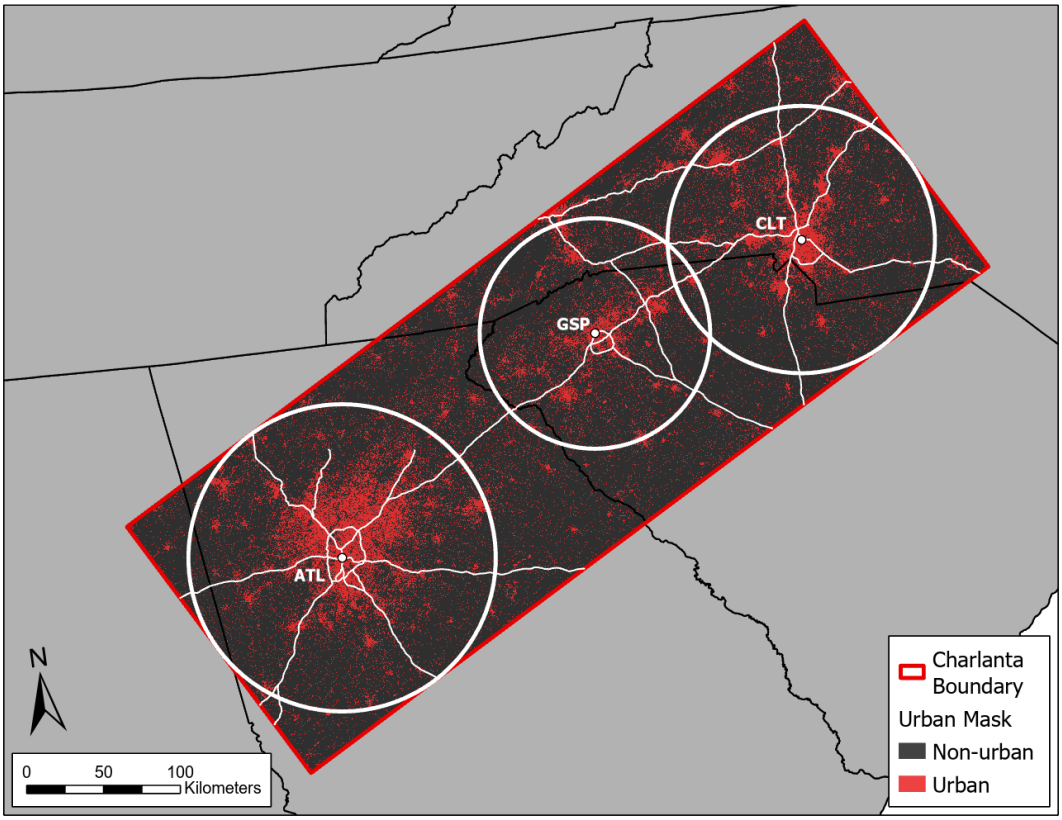

Figure 3.2: Defining the Charlanta megaregion using the minimum bounding geometry of each major city's geometric buffer (white).

3.2.2 Delineating the urban core

In order to delineate the footprint of each city's dense urban core within the outer boundary for statistical analysis, a binary classification method was applied to the NLDN and GLM grid cells utilizing land use and cover (LULC) areal coverage information from the NLCD. Each of the four urban land cover classifications in the NLCD dataset were aggregated to form a broad urban-rural percentage. For each grid cell, if the areal coverage of the urban classes was greater than or equal to 50% of the total cell area, the cell was classified as "urban," while cells with less than 50% coverage were classified as "rural." Finally, cells that were classified as urban but disconnected from the urban core were removed, resulting in a set of conterminous urban cells nested within the outer "rural" boundary of each city (as shown in Figure 3.3 below). In addition to this NLCD-based urban delineation, a more primitive set of urban geometric buffers were also constructed through visual analysis of the developed land classes within each domain. Similar to Ashley et al. (2012), this allowed for comparison between different conceptualizations of the urban-rural boundary.

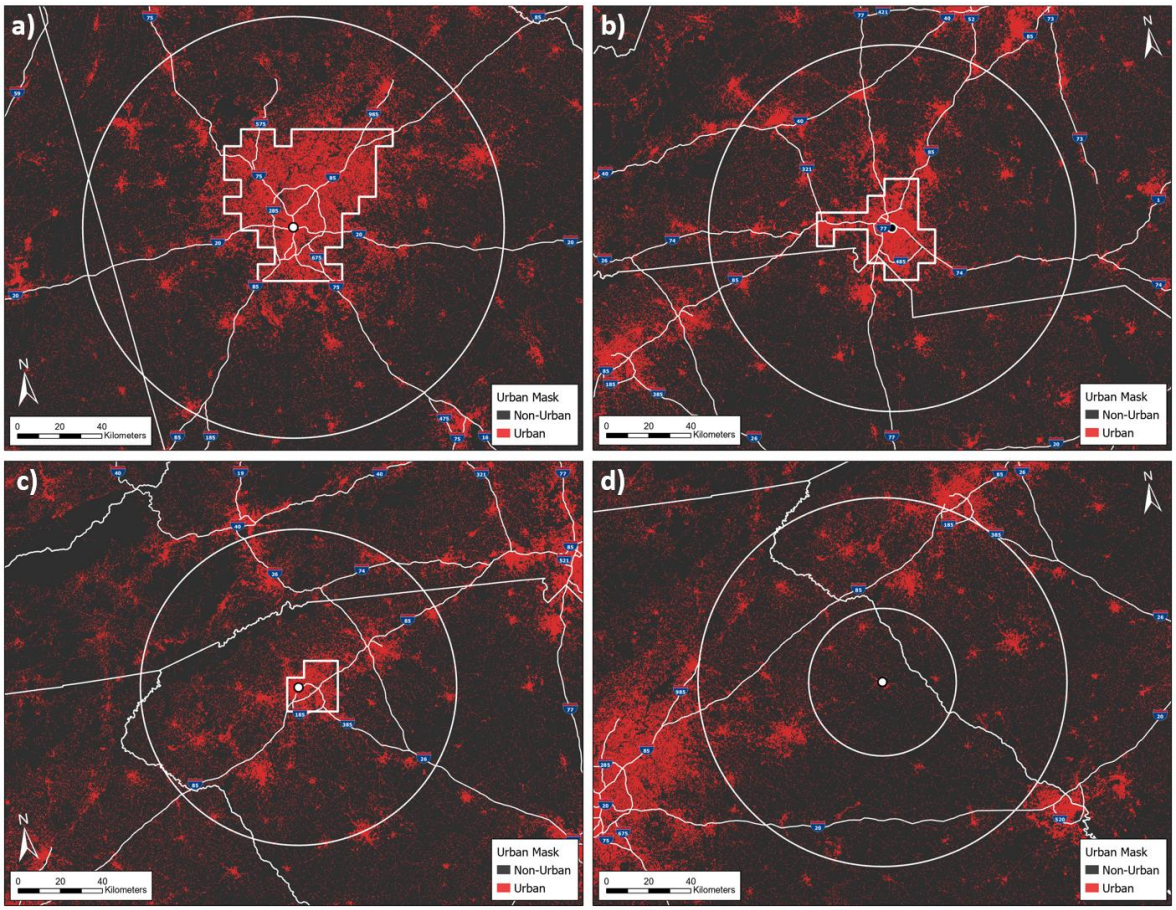

Figure 3.3: NLCD-based urban delineations constructed on the GLM grid to define the domains of (**a**) Atlanta, (**b**) Charlotte, and (**c**) Greenville. (**d**) Surrogate urban buffer created for the Elberton (control) domain. The base urban mask layer was derived from the 2011 NLCD land cover classification.

To facilitate a comparative analysis with the predominantly rural control domain, a surrogate urban buffer was created using an average of the spatial extent of the urban regions from the three cities. As noted by Ashley et al. (2012) and Shepherd (2005), control, or null, regions allowed for validation of the significance of urban flash patterns relative to rural flash patterns. Practically, the purpose of utilizing a rural control domain is to assess the significance of the flash anomalies observed in and around the urban regions i.e., if the rural domain displays

different (similar) lightning hotspots than those discovered in the urban domains, it points towards the significance (insignificance) of urban forcing mechanisms.

3.2.3 Mapping of lightning datasets for visual analysis

After processing in R, the NLDN CG and GLM TL datasets were imported into ArcGIS Pro for further manipulation and creation of the maps required for visual analysis. The prepared CG lightning CSV file was loaded as a feature layer, converted to raster format in which each latitude-longitude point represented a cell's center (0.1° x 0.1° resolution), and projected to the Albers Equal-Area Conic (AEAC) projection (Snyder, 1987), resulting in a spatial resolution of approximately 10 km. Similarly, the GLM TL netCDF4 file was loaded using ArcGIS Pro's *Make NetCDF Feature Layer* tool, converted to raster format in which each latitude-longitude point represented a cell's center (0.08° x 0.08° resolution), and projected to the AEAC projection, resulting in a spatial resolution of approximately 8 km. Finally, the raster layers for each CG and TL metric were clipped to the boundary features defining each city-scale domain and the Charlanta megaregion using ArcGIS Pro's *Clip Raster* tool.

Following preparation of the geographic datasets, maps of each CG and TL metric were created for the four city-scale domains and for the entire Charlanta megaregion. Each of the maps were visually analyzed to determine the apparent spatial patterns of urban lightning augmentation at the city scale and megaregion scale. Special attention was paid to the rural control region, as in theory it should have provided a relative baseline representing patterns of lightning frequency not influenced by urban surfaces. As noted by Ashley et al. (2012), outside controls such as predominant mesoscale circulations and the underlying orographic arrangement of each domain often have an effect on the patterns observed. Consequently, these factors were strongly considered during visual inspection of the mapped CG and TL climatologies.

3.2.4 Quantitative analysis

Following the subjective, visual examination of the mapped CG and TL climatologies, three quantitative analyses were conducted using R to provide a more objective assessment of urban influences on flash production. First, a graphical analysis similar to that of Ashley et al. (2012) and Shepherd et al. (2018) was conducted in which quadratic regression was performed on the data contained by the grid cells within the city scale domains to model the relationship between each TL metric and the distance from city-center. Next, the means of each lightning metric within the urban delineations (primitive geometric and NLCD-based) were compared with those in the outer rural regions to determine the percentage change across each city's domain. Finally, inferential statistical analyses in the form of independent two-sample *t* tests (Mann-Whitney *U* tests) were conducted, utilizing the aforementioned conceptualizations of the urban-rural boundary as sampling schema for each of the four domains (Student, 1908; Mann and Whitney, 1947). More specifically, these tests allowed for an assessment of whether the mean (median) of each CG and TL metric within the urban core of each city displayed a statistically significant difference when compared with the surrounding rural region. An alpha level of 0.05 was used for all of the statistical tests. Formally, the hypothesis tested was:

H_0 = There is no significant difference between the urban and rural samples.

H_1 = There is a significant difference between the urban and rural samples.

Following statistical testing for significant differences between the urban-rural samples at the city-scale, analysis of variance (ANOVA) was performed for each of the urban core delineations to provide a robust assessment of the inter-city variance of each CG and TL metric in the Charlanta megaregion (Kaufmann and Schering, 2014). Tukey's honest significant

difference (HSD) tests were utilized to assess which cities displayed statistically significant differences in the analyzed lightning metrics (Tukey, 1949). Again, the rural control region served as a valuable baseline for validation of the urban enhancement hypothesis.

CHAPTER 4

RESULTS AND DISCUSSION

4.1 Visual analysis

4.1.1 Atlanta, GA

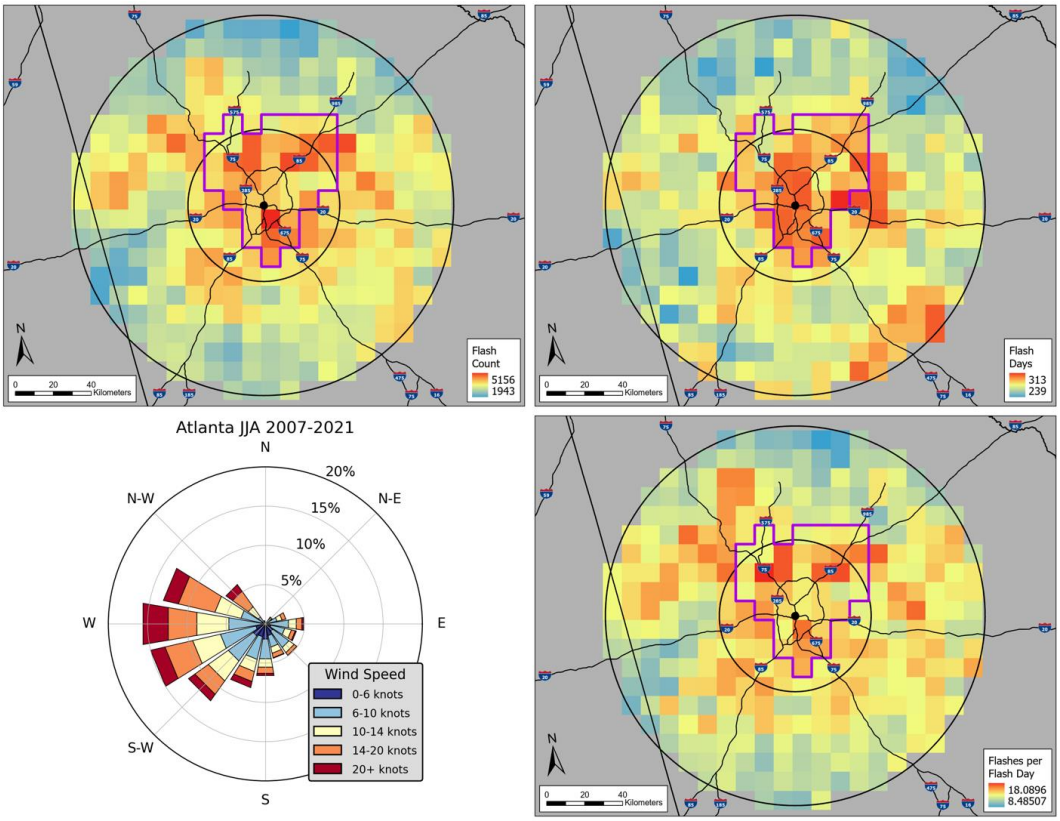

Figure 4.1: Warm season CG flash climatology (2007–2021) overlaid with the aggregated 2011 NLCD urban delineation for the Atlanta domain. Wind rose diagram derived from ERA5 daily average wind speed and direction reanalysis.

The CG flash climatology constructed for the Atlanta domain (shown in Figure 4.1 above) displayed several conspicuous patterns. Hotspots in CG flash count and flashes per flash day were visible to the immediate northwest, northeast, and near the southern extent of the I-285

perimeter. As observed by Ashley et al. (2012), the strongest CG flash intensity hotspots were spatially correlated with the sprawling urban footprint extending outward along Atlanta's main interstate arteries. Another feature to note was the southwest-to-northeast oriented band of elevated flash counts and flashes per flash day further to the northwest of the city center. This was possibly driven by underlying topographic forcing, though emissions from Plant Bowen, a coal-fired power station in Euharlee, GA (Patrinos et al., 1978; *Plant Bowen Info Sheet*, 2016), may have also contributed to locally enhanced flash production (Debbage et al., 2015; Strikas and Elsner, 2013). In contrast to the distributions of the CG flash intensity metrics, flash days were more strongly concentrated over the central extent of the urban core and immediately to the east of the I-285 perimeter, roughly following I-20. Near the southeastern boundary of the domain, there was an area of elevated flash days likely associated with the disparate surface topography and resultant differential heating along the Atlantic fall line which promotes thunderstorm development, as noted by Miller and Mote (2017) in their climatological analysis of WFTs in the Southeast.

The Atlanta TL climatology derived from GLM group data (displayed in Figure 4.2 below) exhibited more distinct, isolated patterns of probable urban augmentation. A concentrated hotspot in group count and groups per group day was visible to the northeast of the city center (near the junction of I-85 and I-985), with a connected arc of elevated values extending approximately 75 km to the east and along I-20 to the south. This downwind arc of anomalous TL intensity was noticeably further east than the downwind anomaly observed in the CG intensity climatology. Other notable hotspots in TL intensity were located within the core area of urban development, to the immediate west-southwest of the I-285 perimeter and near the south-southwestern extent of the domain. TL frequency at the daily scale, quantified by the group days

metric, displayed hotspots over the south-central core of the city and near the northernmost extent of the domain, likely associated with the rising terrain of the Blue Ridge mountains. Additionally, there were patches of elevated group day totals across the northern half of the core region and roughly following I-20 downwind of the city. In general, TL group days were most strongly clustered within 40 km of the city center, though the urban signal was seemingly weaker than that observed in the CG flash climatologies.

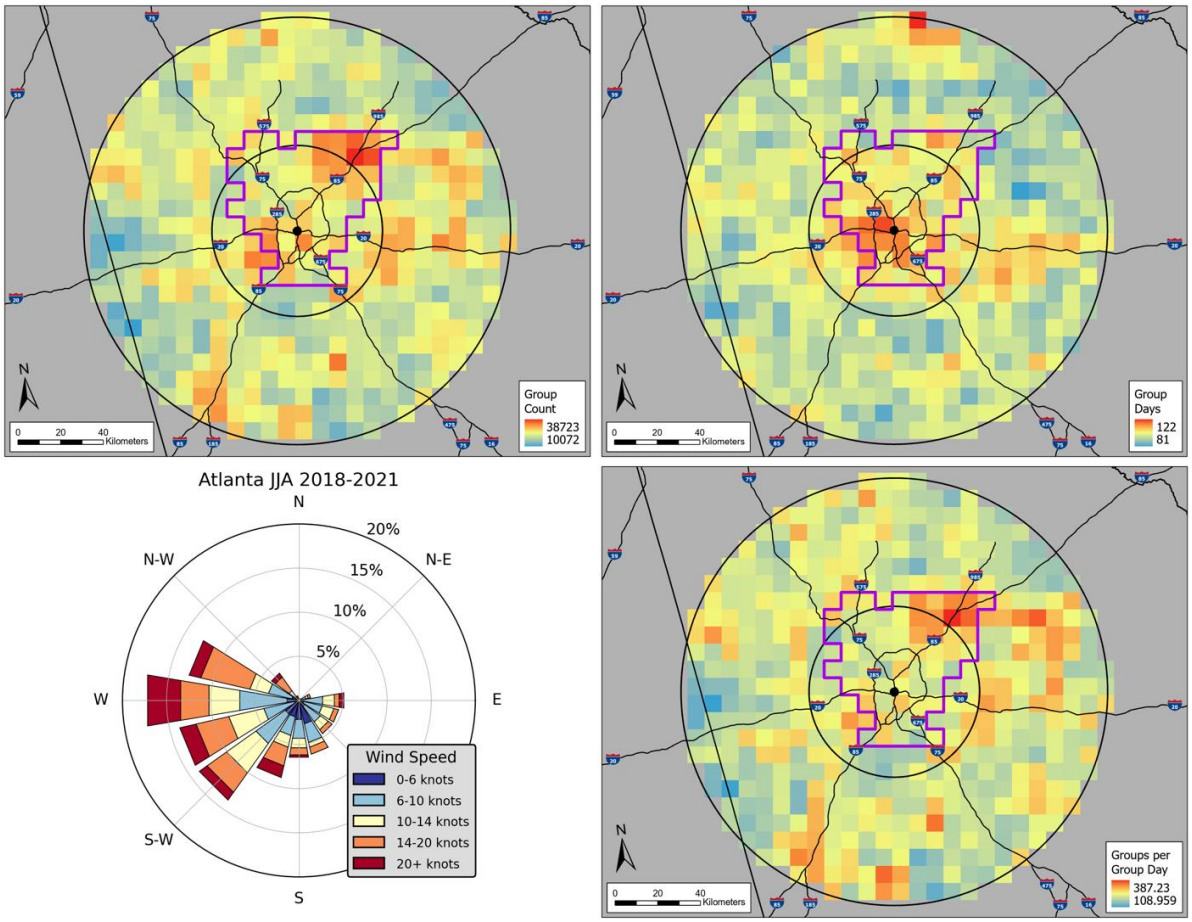

Figure 4.2: Warm season TL (GLM group) climatology (2018–2021) overlaid with the aggregated 2011 NLCD urban delineation for the Atlanta domain. Wind rose diagram derived from ERA5 daily average wind speed and direction reanalysis.

As expected, the well-documented enhancement of lightning intensity and frequency over and downwind of the urban core appeared in both of the CG and TL climatologies. Furthermore, the oft-observed hotspot to the northeast of Atlanta's I-285 perimeter is also present in both CG and TL climatologies, aligning with the results of previous studies analyzing lightning and precipitation (Diem and Mote, 2005; McLeod and Shepherd, 2022; McLeod et al., 2017). As noted by Stallins (2004), this downwind-upwind pattern of augmentation is expected to evolve as land cover distributions change, modifying the role of urban forcings. Additionally, the persistent observation of elevated CG and TL intensity extending from Atlanta's core to the west-southwest, roughly following Interstate-85, presents the possibility that the terrain of the Chattahoochee River Valley (displayed in Figure 4.3 below) is an important factor in proximal convective activity. Westcott (1995) and McLeod et al. (2017) hypothesized that this mechanism of topographically driven enhancement may result in a preferred area of downwind convective activity.

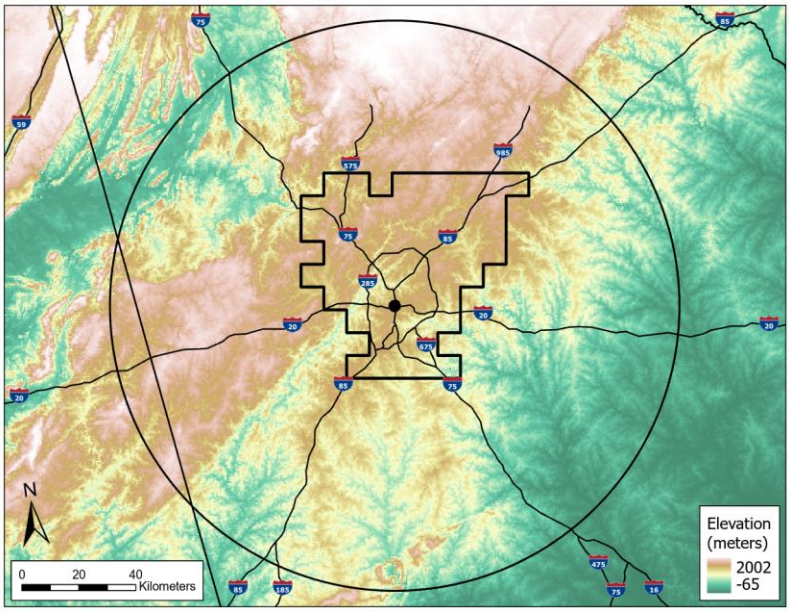

Figure 4.3: Topography of the Atlanta domain overlaid with the outer rural boundary and inner NLCD-based urban core delineation. Mean elevation of each pixel displayed in meters.

4.1.2 Charlotte, NC

As displayed in Figure 4.4, the dominant hotspot in CG flash count and flashes per flash day is tightly concentrated within and immediately downwind of Charlotte's urban core, though a broad area of elevated flash counts is observable along the southern extent of the domain. Isolated areas of elevated values in all three CG flash metrics lie to the west and northwest of the city, likely associated with terrain features depicted in Figure 4.7. While CG flash days are also elevated near the city-center relative to the immediate rural surroundings, the most prominent hotspot is spatially coincident with the aforementioned flash count anomaly near the south-southeastern periphery. This extraneous band of elevated CG flash counts and days at the southern extent is presumably a result of local physiographic features that promote both free and forced convection, namely, the Carolina Sandhills and the Catawba River Valley (Sims and Raman, 2016; Wooten et al., 2010). Demonstrating the essential utility of the metric, the absence of a spatially coincident hotspot in CG flashes per flash day indicates that the observed flash count anomaly is predominantly a result of more frequent thunderstorms at the daily scale, rather than more productive thunderstorms with regard to flash rates. Conversely, the observation of a concentrated hotspot in CG flashes per flash day located over Charlotte's core region indicates the city's role in modifying flash production is manifested most prominently at the daily storm-scale, with the average CG flash day near the urban core tending to be more electrically active than in the surrounding areas.

In contrast to the Atlanta TL climatology displayed in Figure 4.2, that developed for Charlotte (shown in Figure 4.6 below) exhibited a markedly weaker and less distinct urban signal. The distributions of TL group count and groups per group day, both aiming to represent TL intensity, contained concentrated anomalies to the immediate north-northeast of the urban

core roughly following the I-85 corridor. While it is quite possible these anomalies are associated with the typical downwind augmentation process, the heterogeneity of the underlying surface characteristics must be considered as another contributor. Likewise, the daily frequency of TL, represented by the group days metric, appeared to be heavily influenced by the terrain features of the Blue Ridge Mountains across the northwestern half of the domain (displayed in Figure 4.7). In contrast to Charlotte's CG flash climatology, no substantial anomaly was observed in any of the TL metrics along the southern extent of the domain.

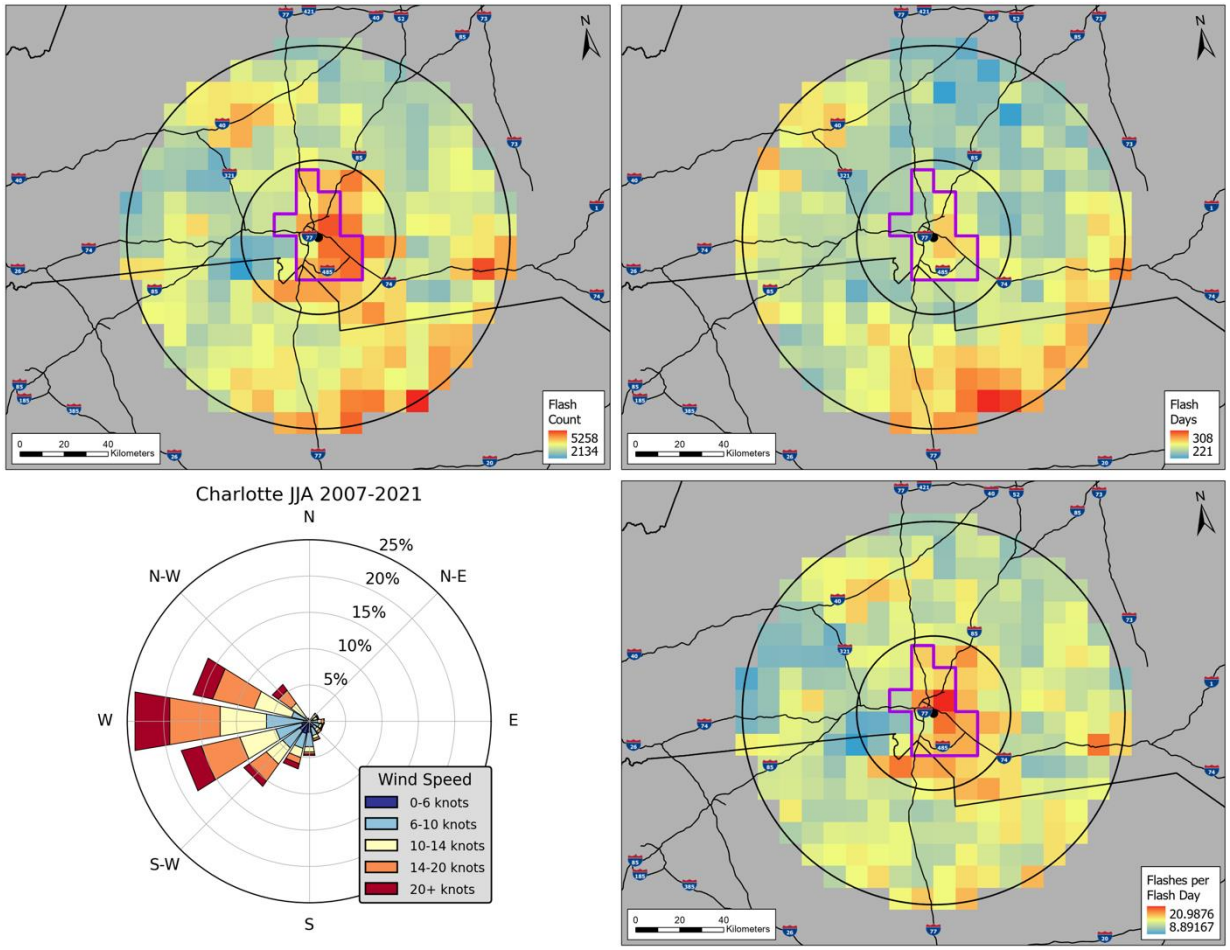

Figure 4.4: Warm season CG flash climatology (2007–2021) overlaid with the aggregated 2011 NLCD urban delineation for the Charlotte domain. Wind rose diagram derived from ERA5 daily average wind speed and direction reanalysis.

The disparity between Charlotte's CG and TL climatologies near the south-southeastern periphery highlights the need for more intensive research into the complex factors that determine the observed preference for CG lightning production in the area. Relevant meso-analyses conducted by Sims and Raman (2016, 2019) investigated the interactions between the shallow density currents produced by Sandhills-driven convection and the diurnally driven sea-breeze circulations that occur along the Atlantic coastline. A schematic of this process is displayed in Figure 4.5 below. Nevertheless, though the sea-breeze front in this region has been shown to travel as far as 150 km inland (Koch and Ray, 1997), the peripheral area of the Charlotte domain defined in this study is approximately 165 km from the coast, preventing these interactions from being a consistent factor in the production of the CG flash count and day anomalies. Therefore, it is most probable that the anomaly results primarily from deep convection over the Sandhills (depicted in Figure 4.5 as the maroon arrow at left).

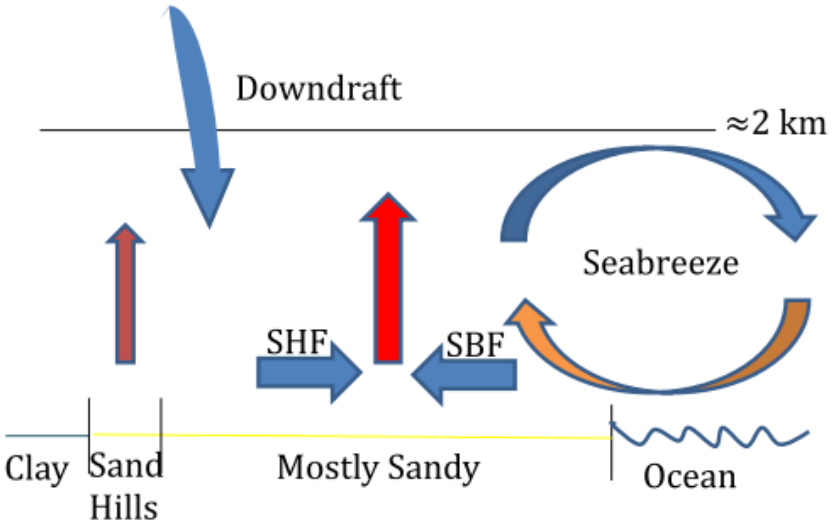

Figure 4.5 Depiction of the interaction between the Sandhills front (SHF) propagating east-southeast and the sea-breeze front (SBF) propagating west-northwest from Sims and Raman (2019). Note: diagram is not to scale.

While the research of Sims and Raman (2016, 2019) focused on the SHF propagating to the east-southeast, the corresponding front propagating to the west-northwest is of greater importance to analyses focused on the city of Charlotte. Summarizing the theory being suggested, is it possible that this SHF contributes to convective enhancement and related lightning production over Charlotte's urban core? Furthermore, is there a potential interaction between this process and BLHI-induced meso-circulations driven by Charlotte's core area of development? These questions further emphasize the need for more localized investigations and numerical modeling analysis of convective enhancement in the greater Charlotte metropolitan area.

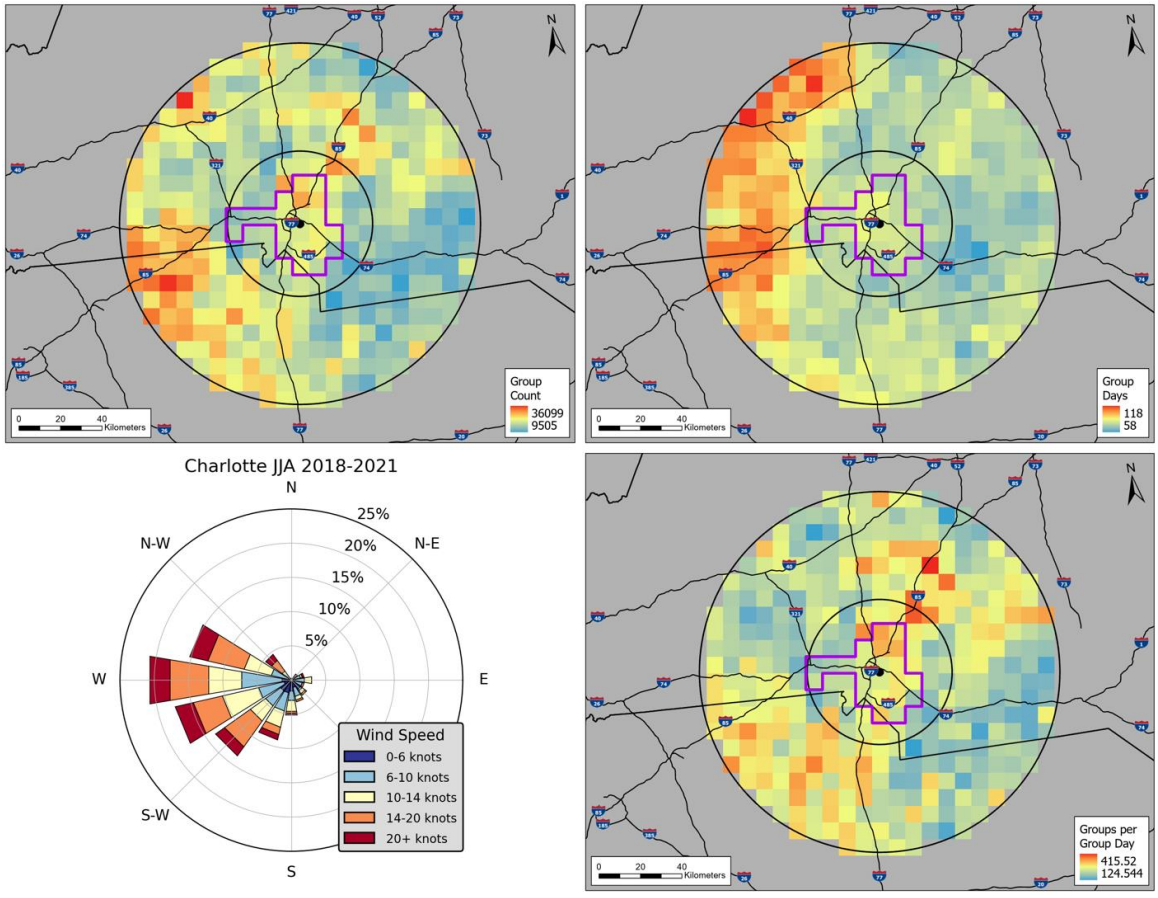

Figure 4.6: Warm season TL (GLM group) climatology (2018–2021) overlaid with the aggregated 2011 NLCD urban delineation for the Charlotte domain. Wind rose diagram derived from ERA5 daily average wind speed and direction reanalysis.

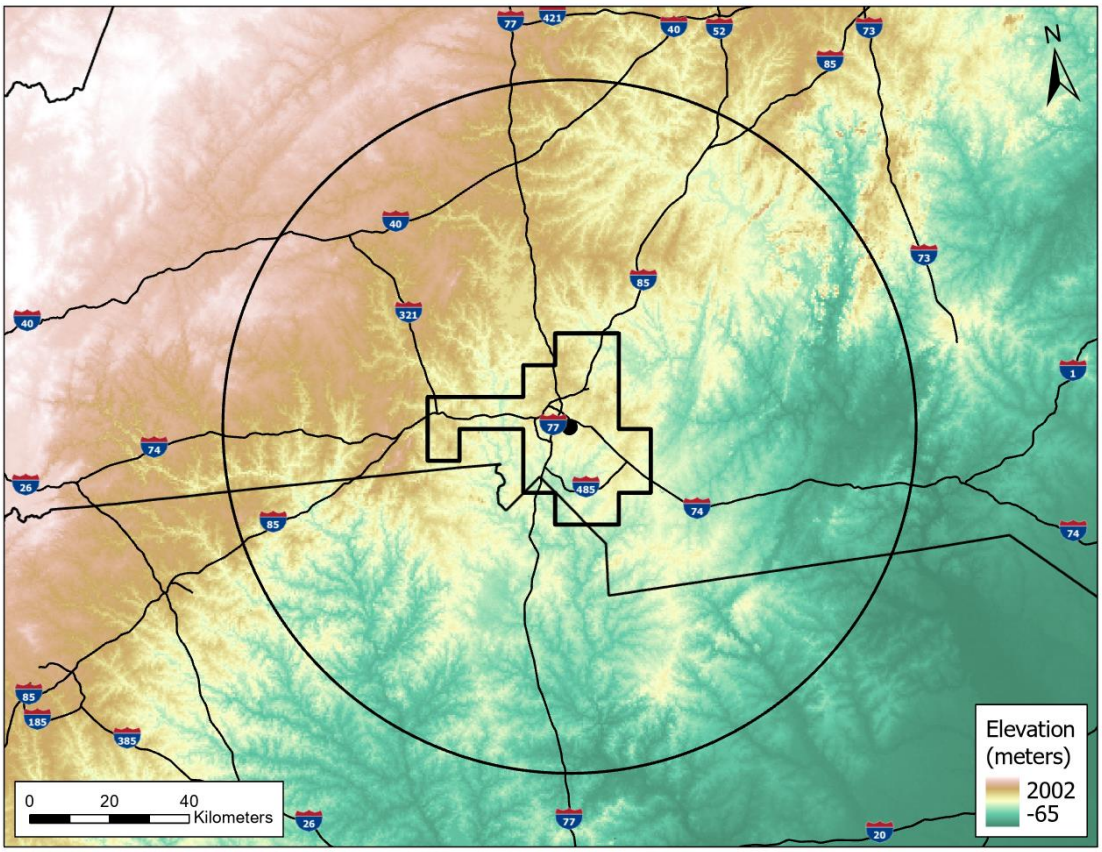

Figure 4.7: Topography of the Charlotte domain overlaid with the outer rural boundary and inner NLCD-based urban core delineation. Mean elevation of each pixel displayed in meters.

4.1.3 Greenville, SC

The more moderately sized city of Greenville displayed a weaker and more inconspicuous urban influence, with elevated CG flash counts distributed broadly across the northern half of the domain, and a distinct non-urban CG flash days hot spot in the northwestern quadrant of the outer buffer. It is probable that the latter is connected to the local topography as this area of the Greenville domain extends into the rising terrain of the Blue Ridge mountains. Most notable, though, was the region of elevated CG flashes per flash day extending from the city's core to the northeast, roughly following the I-85 corridor past Spartanburg, SC and reaching its greatest intensity near the extent of the rural buffer. Indicative of more active

thunderstorms with regard to flash production, this situation demonstrates another utility of the flashes per flash day metric in revealing a potential urban signal in the lightning distributions of small to moderately sized cities. Although well outside the demarcated urban core of Greenville, the landscape within this corridor is generally downwind and consists of substantial urban sprawl connecting the cities of Greenville and Spartanburg.

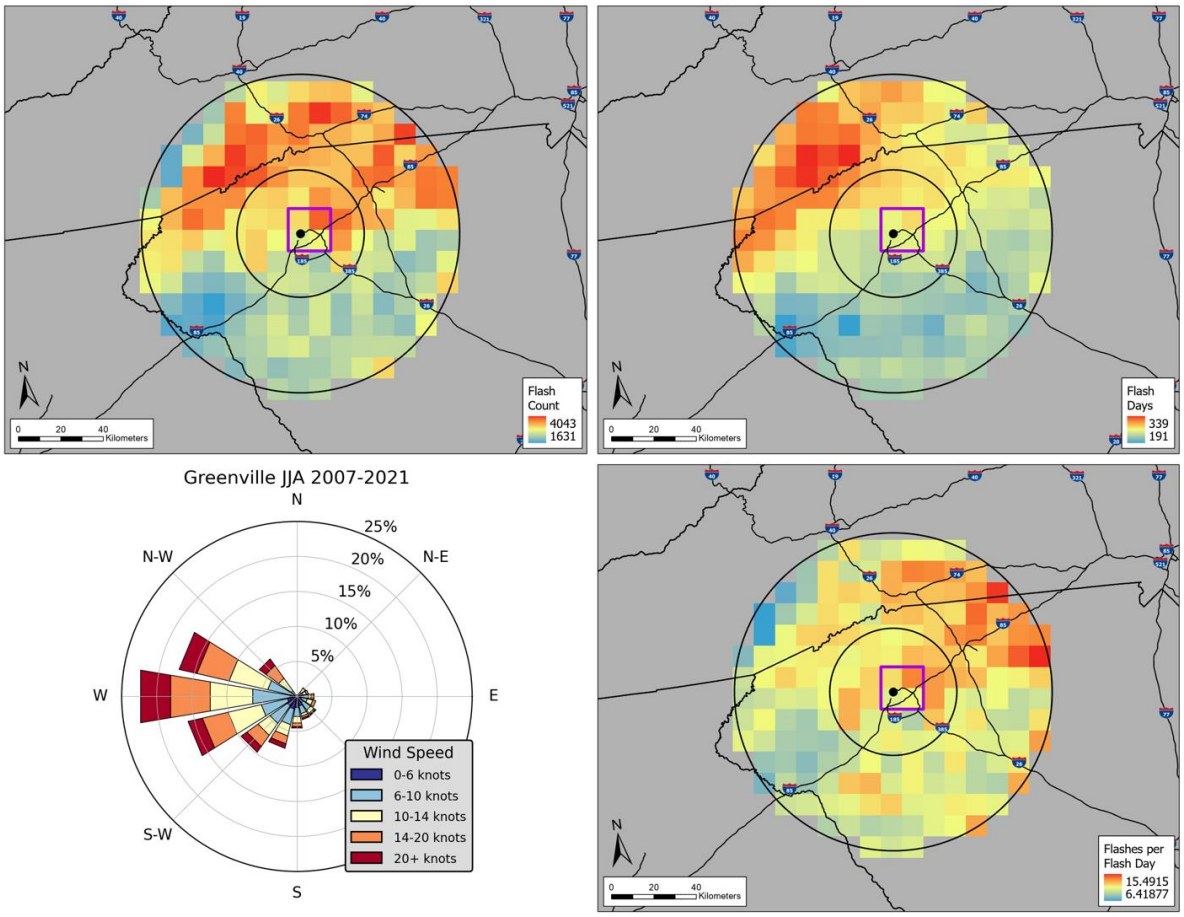

Figure 4.8: Warm season CG flash climatology (2007–2021) overlaid with the aggregated 2011 NLCD urban delineation for the Greenville domain. Wind rose diagram derived from ERA5 daily average wind speed and direction reanalysis.

As with the CG climatology, the TL climatology for Greenville displayed terrain-influenced hot spots in group count and group days to the immediate northwest of the core and near the northernmost extent of the domain. There were isolated hot spots in group count and

groups per group day to the immediate west of Greenville's NLCD-based core delineation, and to the southwest and east-southeast of the core geometric buffer. Unlike the CG climatologies, a cold spot was observed over and to the immediate northeast of the urban core, an area that is typically downwind based on the displayed wind rose climatology. The smaller size and spatial density of the Greenville metro area underlies an expectation that its urban influences will be weaker relative to geophysical controls on lightning production. Nevertheless, urban forcings likely act in a supplementary capacity. Consequently, the observed hotspots in flashes (groups) per flash (group) day demonstrate the need for further investigation using a methodology tailored to a twin-cities layout and with higher resolution lightning data.

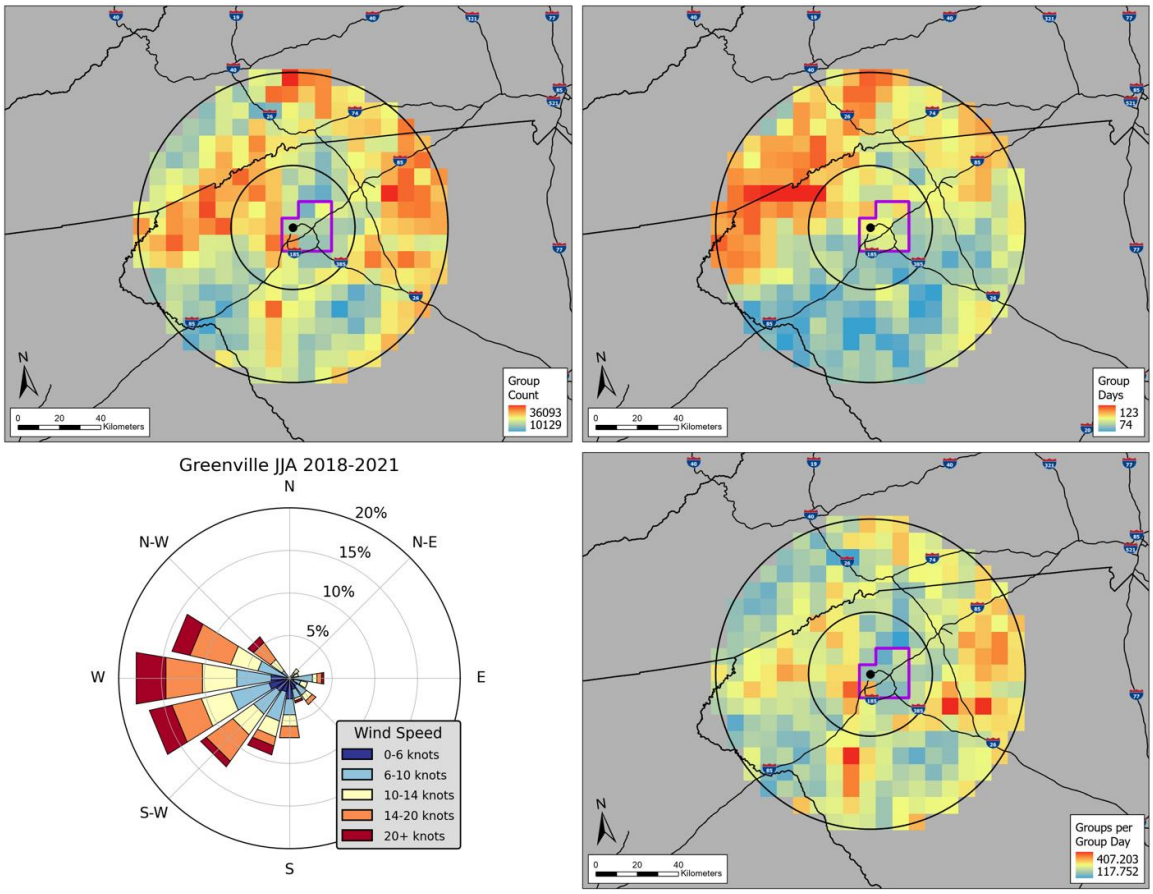

Figure 4.9: Warm season TL (GLM group) climatology (2018–2021) overlaid with the aggregated 2011 NLCD urban delineation for the Greenville domain. Wind rose diagram derived from ERA5 daily average wind speed and direction reanalysis.

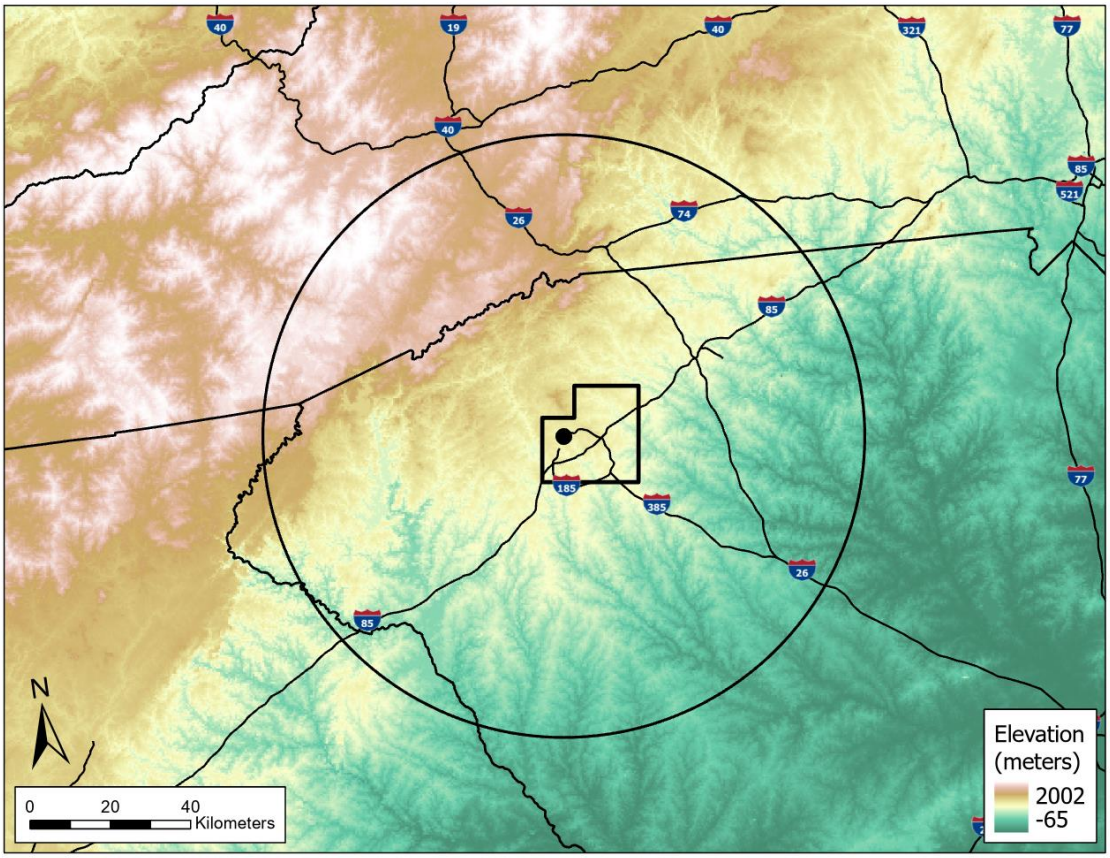

Figure 4.10: Topography of the Greenville domain overlaid with the outer rural boundary and inner NLCD-based urban core delineation. Mean elevation of each pixel displayed in meters.

4.1.4 Elberton, GA

Concluding visual analysis at the city-scale, only TL group days displayed moderately elevated values within the inner buffer of the Elberton control domain, as shown in Figure 4.12 below. The overwhelming predominance of markedly lower values of both CG and TL metrics within the surrogate buffer validates the significance of the urban signal observed around the major cities of Charlanta. A final set of notable features were the hotspots in both CG and TL count and day metrics to the west of the inner buffer that, upon finer inspection, were approximately co-located with the city of Athens, GA.

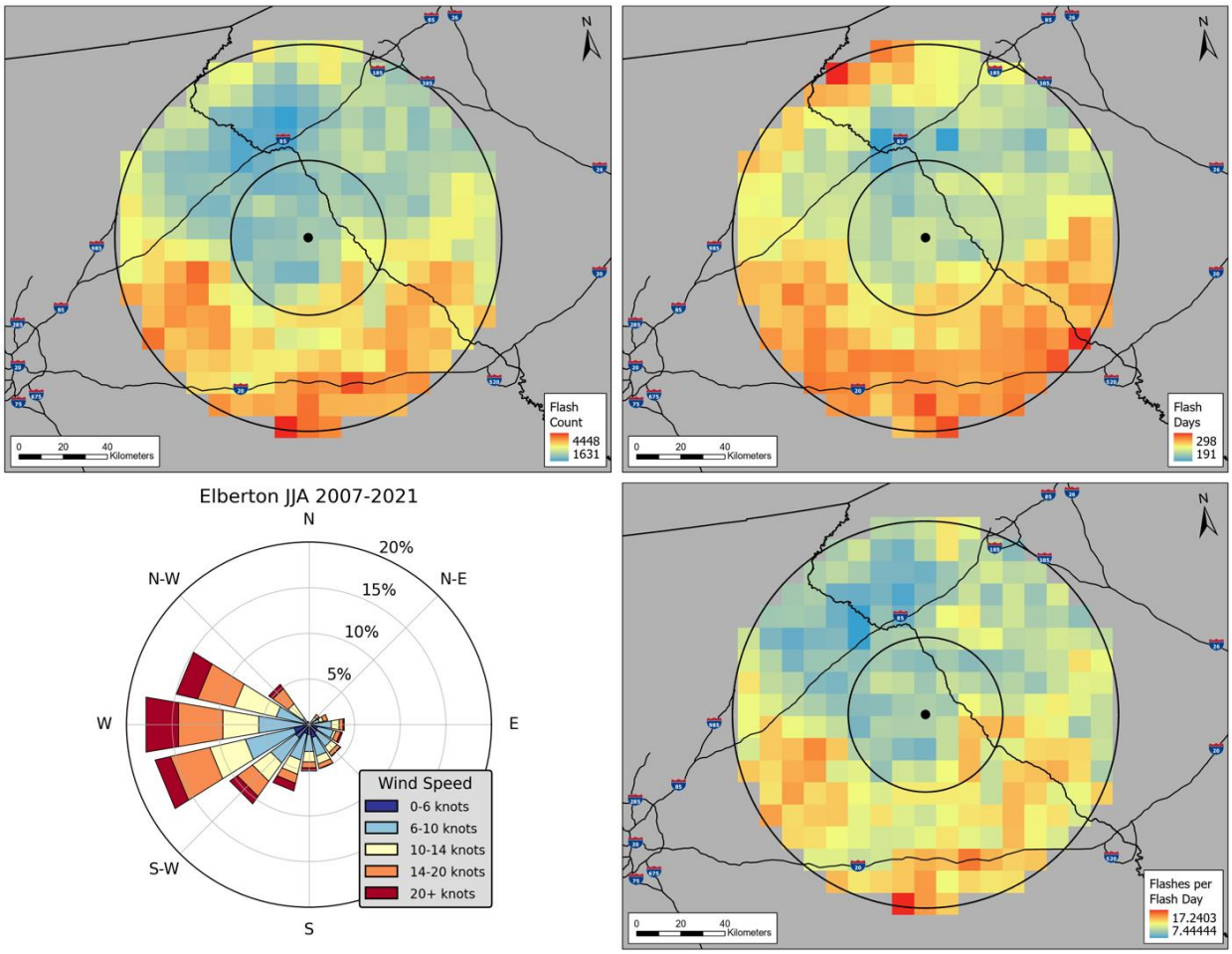

Figure 4.11 Warm season CG flash climatology (2007–2021) overlaid with the surrogate urban buffer for the Elberton domain. Wind rose diagram derived from ERA5 daily average wind speed and direction reanalysis.

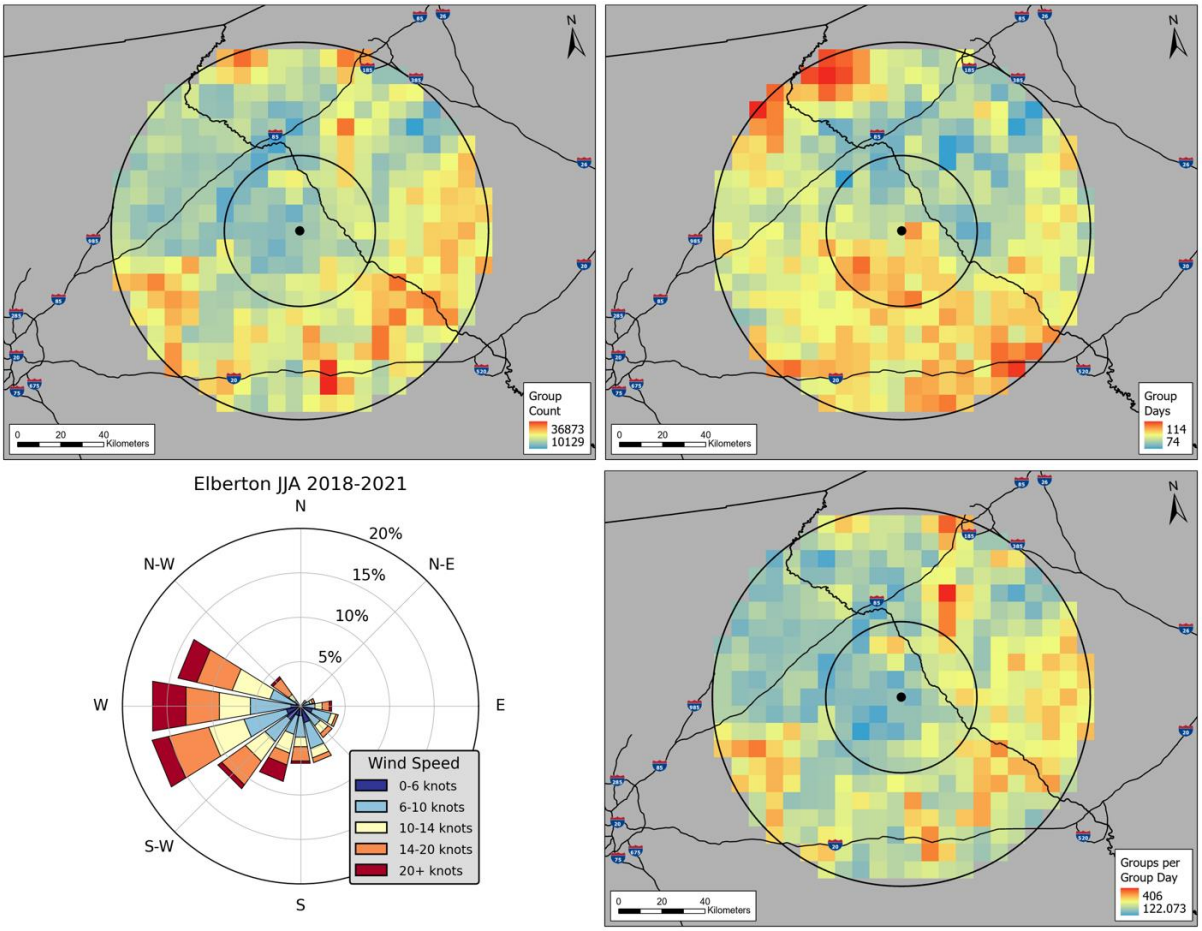

Figure 4.12: Warm season TL (GLM group) climatology (2018–2021) overlaid with the surrogate urban buffer for the Elberton domain. Wind rose diagram derived from ERA5 daily average wind speed and direction reanalysis.

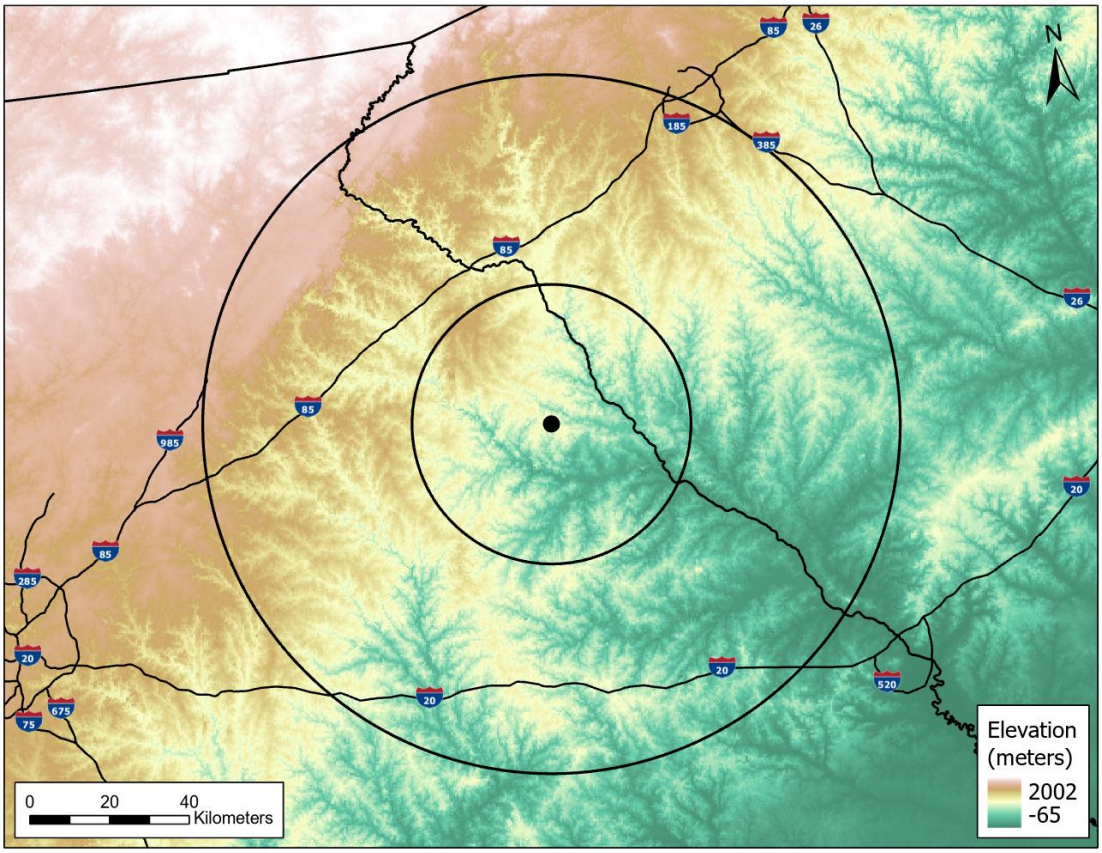

Figure 4.13: Topography of the Elberton domain overlaid with the geometric buffer used to represent a surrogate urban control region. Mean elevation of each pixel displayed in meters.

4.1.5 Megaregion-scale

Visual analysis of the CG and TL climatologies developed for the Charlanta megaregion (displayed in Figures 4.14 and 4.15) highlighted several of the familiar patterns observed at the city-scale, but with additional spatial context endowed by the expanded scope of analysis. The megaregion-scale climatologies provided a more complete view of the topographically driven anomalies in CG and TL frequency along the Blue Ridge Escarpment that were detected in each of the Greenville and Charlotte domains. Both Atlanta and Charlotte continued to exhibit the strongest signal in each of the CG flash metrics, while Greenville's weaker urban influence on CG flash production became even more indistinct, yet still perceptible when viewed at the

megaregion-scale. As observed in the city-scale climatologies, CG flash count and flashes per flash day were more tightly concentrated over the urban core of Charlotte relative to Atlanta. The area of enhanced CG flash frequency to the south-southeast of Charlotte previously hypothesized to be a result of Sandhills-driven convective activity was again coincident with a relative void in each TL metric.

Focusing on the greater Atlanta metropolitan area, a few distinct features were discovered that have not been clearly identified in previous research. Aligning with Atlanta's city-scale CG and TL climatologies, the most apparent novel characteristic of the megaregion-scale climatologies was again the downwind anomaly extending further to the east of the urban core than observed in previous studies in the area. Though more thorough investigations with more focused methodologies are required before such conclusions can be made, these observations lend support to the hypothesis that patterns of the ULE are spatio-temporally evolving as the underlying propulsive mechanisms change through rapid urban expansion and densification. Another set of novel features observed in the greater Atlanta area were the band of elevated CG flash counts to the northwest of the city center and the coincident hotspot in flashes per flash day that were previously identified in the city-scale analyses as the likely results of topographic forcing and emissions from Plant Bowen. Again, as these anomalies were not present in the map of total CG flash days, it is apparent that they were associated with particularly active thunderstorms in terms of lightning production. In similar fashion, the possible promotion of CG and TL intensity by the topography of the Chattahoochee River Valley was again observed in the megaregion-scale climatologies. This pattern was especially prominent in the TL climatology displayed in Figure 4.15, with elevated TL group count and groups per group day seen extending

along Interstate-85 from the urban core to the southwestern boundary of the Charlanta megaregion.

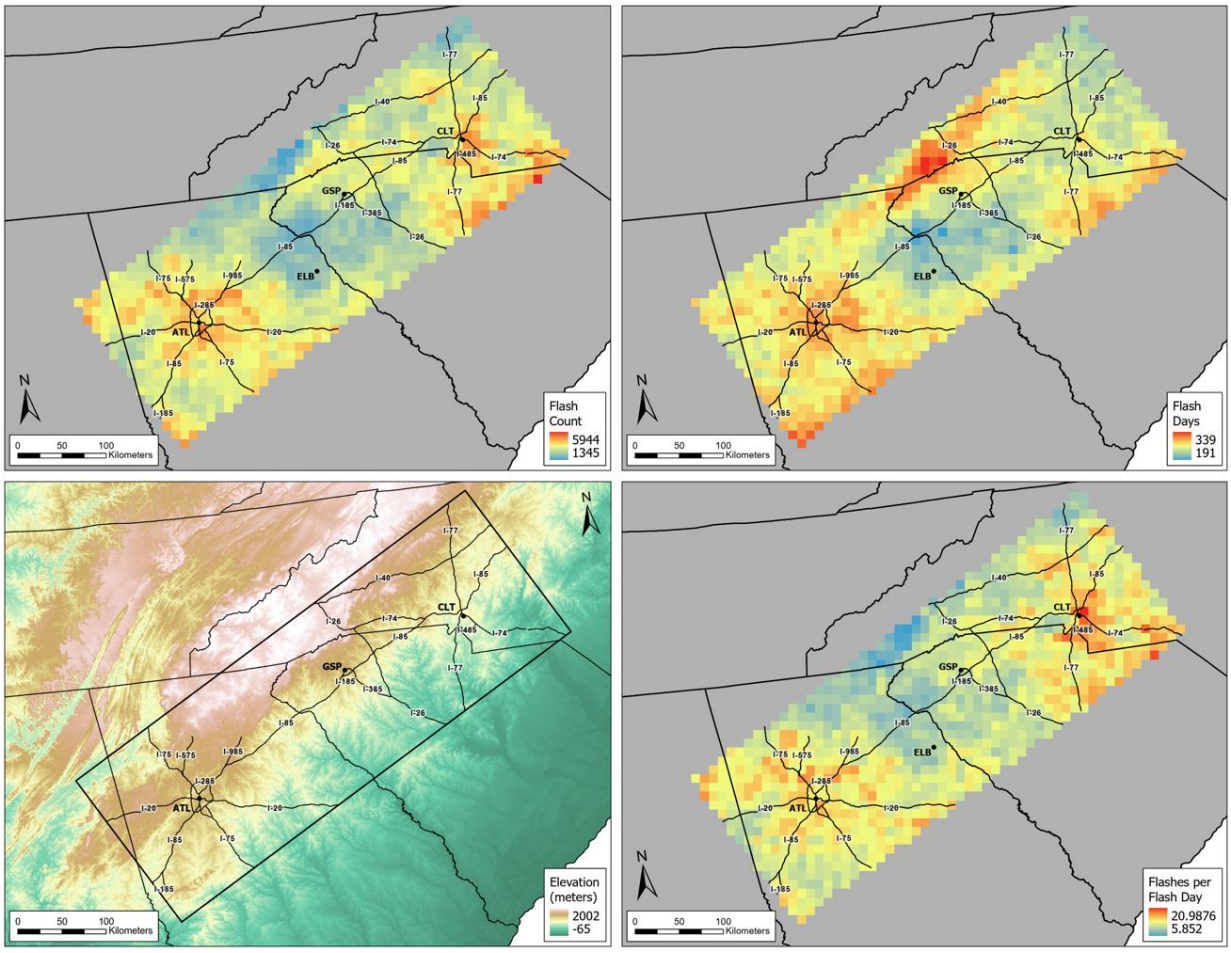

Figure 4.14: Warm season CG flash climatology (2007–2021) and topography across the Charlanta megaregion. Mean elevation within each pixel displayed in meters.

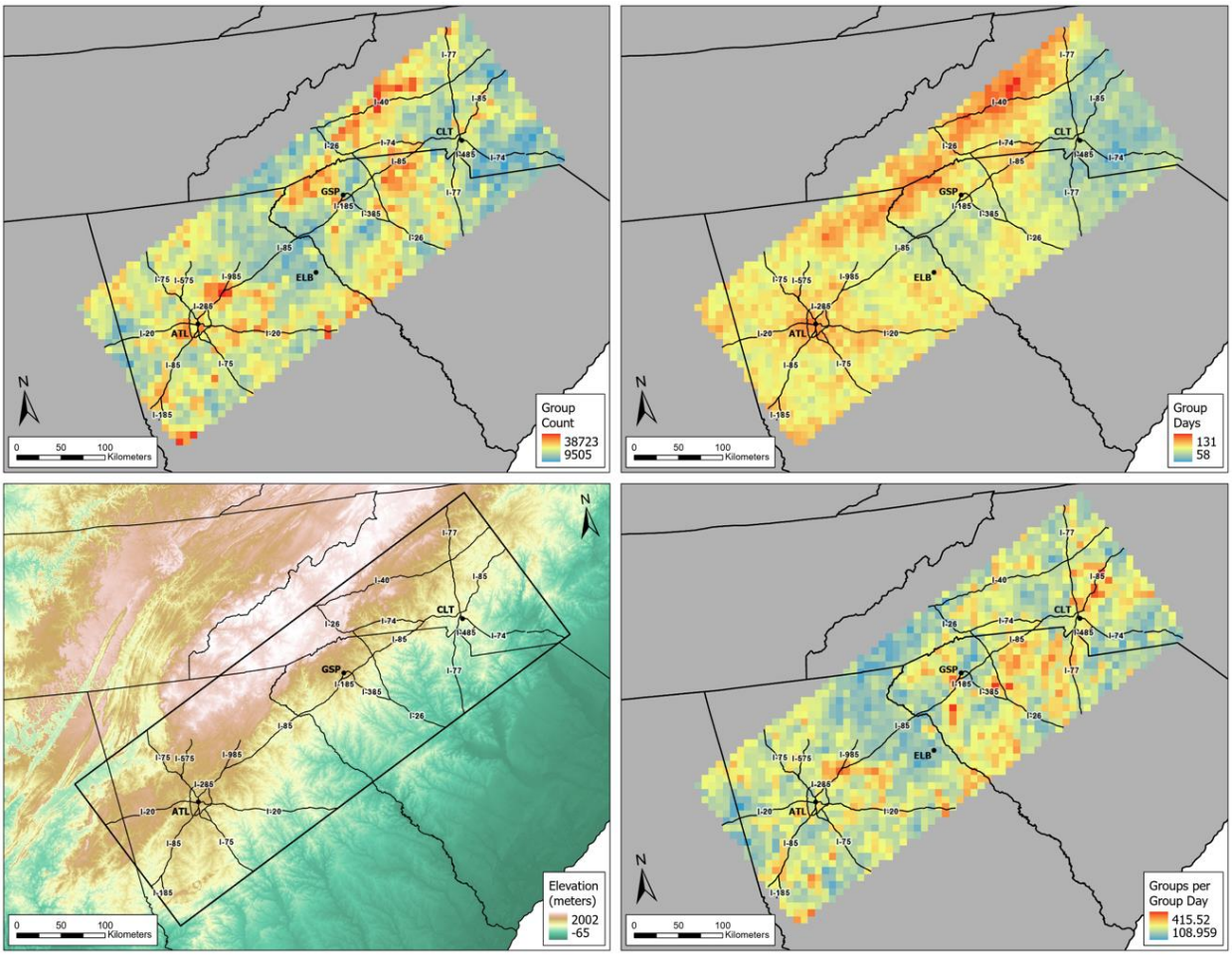

Figure 4.15. Warm season TL group count climatology (2018–2021) and topography across the Charlanta megaregion. Mean elevation within each pixel displayed in meters.

4.2 Quantitative analysis

Building upon the subjective, visual analysis performed in Chapter 4, a set of graphical and statistical analyses were performed on the NLDN CG climatologies and GLM TL climatologies to provide a more objective assessment of urban enhancement in proximity to Charlanta's major cities, specifically over their spatially dense urban cores. In weakly-forced environments like those experienced across the Charlanta megaregion throughout much of the warm season (JJA), the most intense augmentation of CG flash production would be expected

over and near the urban core. There has yet to be an assessment of such influences on distributions of TL, underlying one of the fundamental motivations for this analysis.

4.2.1 Quadratic plots

The results of the graphical analyses of each flash metric displayed in figures 4.16–4.21 below provide additional context to support the findings of the visual analysis. As expected, the Atlanta domain displayed consistent decreases in both CG and TL metrics as the distance from city center increased, though these findings differ slightly from the similar analysis of reflectivity data around Atlanta performed by Ashley et al. (2012) for the years 1997–2006. Each of their fitted quadratic lines exhibited a concave curvilinear shape like that shown in Figure 4.18a for the flash days metric. In contrast, Atlanta's CG and TL count and mean count per day scatterplots displayed more linear and slightly convex shapes, respectively. Along with the results of the megaregion-scale visual analysis, this is potentially an indication that the drastic expansion and coincident densification of developed sprawl across the Atlanta metro area over the past 15 years has altered the spatial extent of its urban influences on flash production.

The graphical results for the Charlotte domain contained quadratic fits more in line with those of Ashley et al. (2012), though the scatterplot for CG (TL) days exhibited an overall increase with distance from city center due to the previously noted topographically driven hotspot across the south-southeastern (west-northwestern) extent of the domain. Greenville's flash count and flashes per flash day fits were particularly interesting as they gradually sloped away from the city center, while the flash days fit was approximately flat. Nevertheless, the de facto twin-city spatial layout of Greenville and neighboring Spartanburg is a confounding factor that makes this form of analysis less informative for accurately determining urban influences.

Lastly, the quadratic fits for the Elberton control domain were all sloped towards the city center, reaffirming the significance of the urban patterns detected in the other domains.

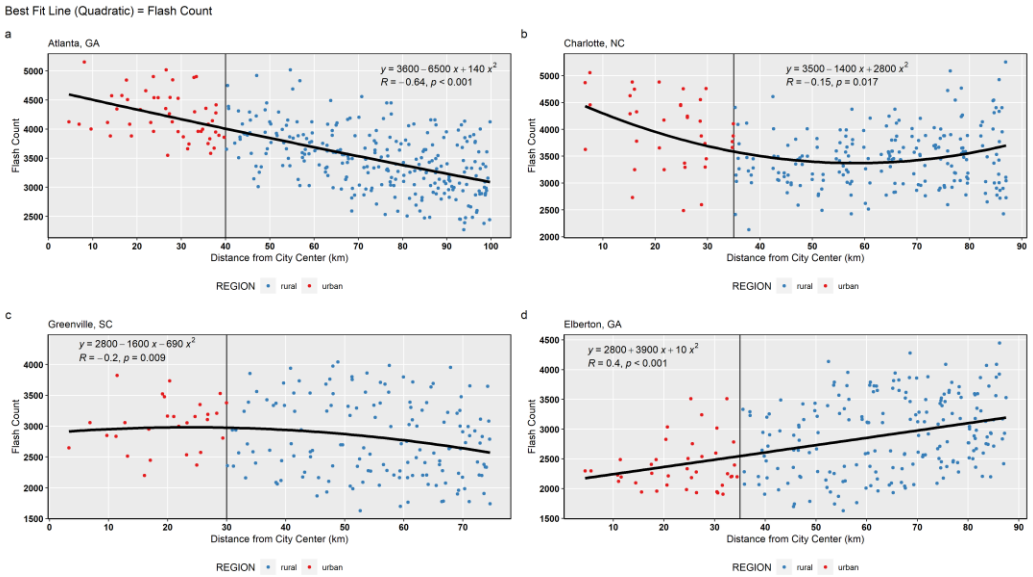

Figure 4.16: Scatterplots and quadratic line fits of warm season CG flash count versus distance from city center for the (**a**) Atlanta, (**b**) Charlotte, (**c**) Greenville, and (**d**) Elberton (control) domains over the 15-year study period (2007–2021).

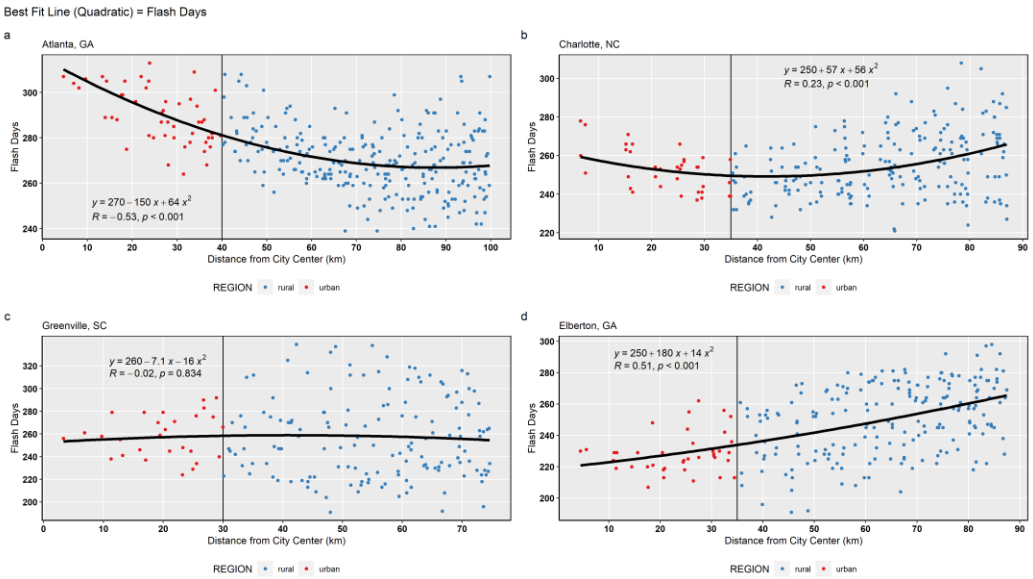

Figure 4.17: Scatterplots and quadratic line fits of warm season CG flash days versus distance from city center for the (**a**) Atlanta, (**b**) Charlotte, (**c**) Greenville, and (**d**) Elberton (control) domains over the 15-year study period (2007–2021).

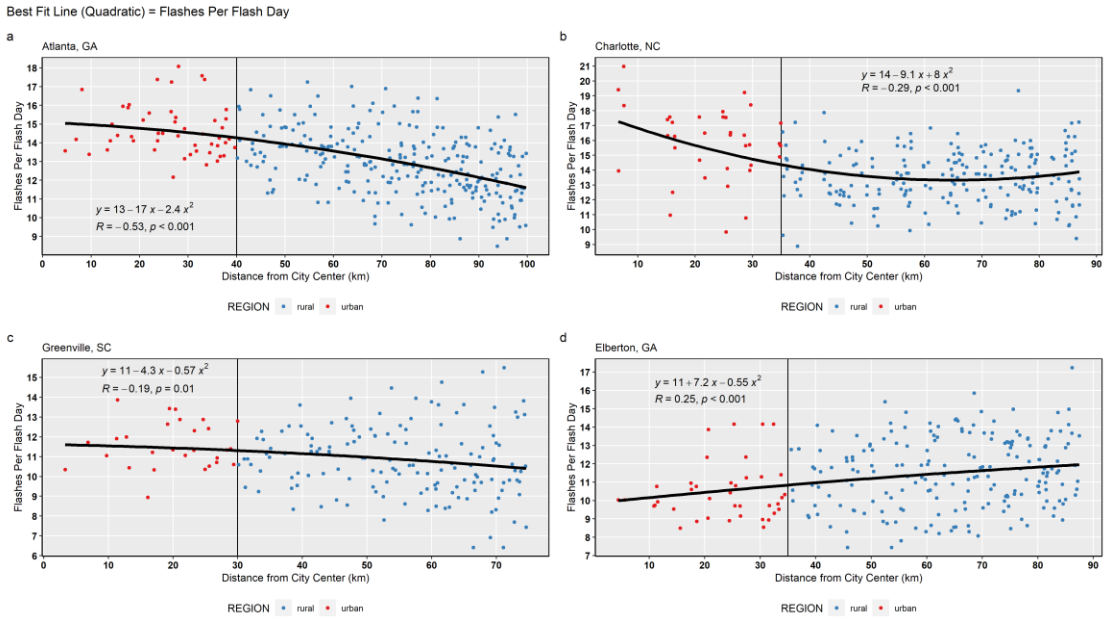

Figure 4.18: Scatterplots and quadratic line fits of mean warm season CG flashes per flash day versus distance from city center for the (**a**) Atlanta, (**b**) Charlotte, (**c**) Greenville, and (**d**) Elberton (control) domains over the 15-year study period (2007–2021).

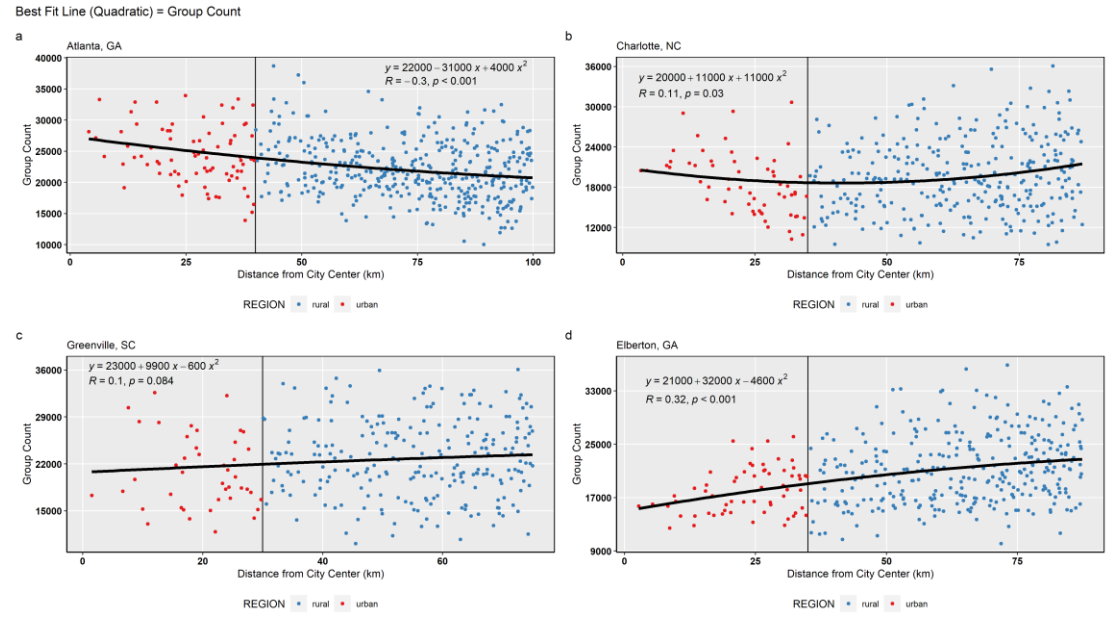

Figure 4.19: Scatterplots and quadratic line fits of warm season TL group count versus distance from city center for the (**a**) Atlanta, (**b**) Charlotte, (**c**) Greenville, and (**d**) Elberton (control) domains over the 4-year study period (2018–2021).

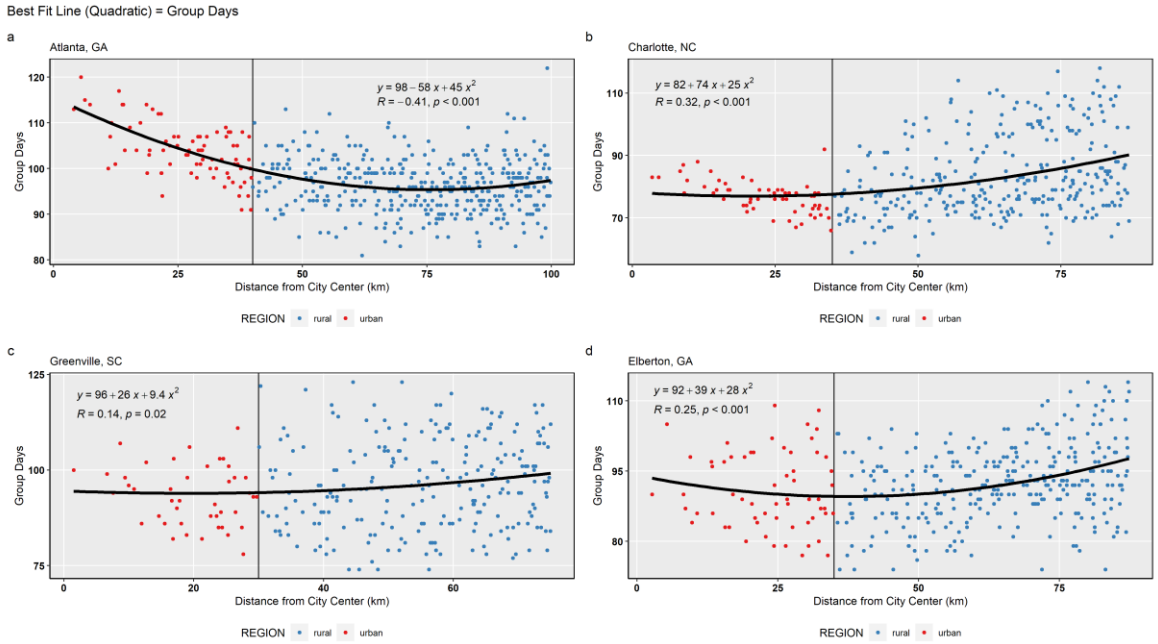

Figure 4.20: Scatterplots and quadratic line fits of warm season TL group days versus distance from city center for the (**a**) Atlanta, (**b**) Charlotte, (**c**) Greenville, and (**d**) Elberton (control) domains over the 4-year study period (2018–2021).

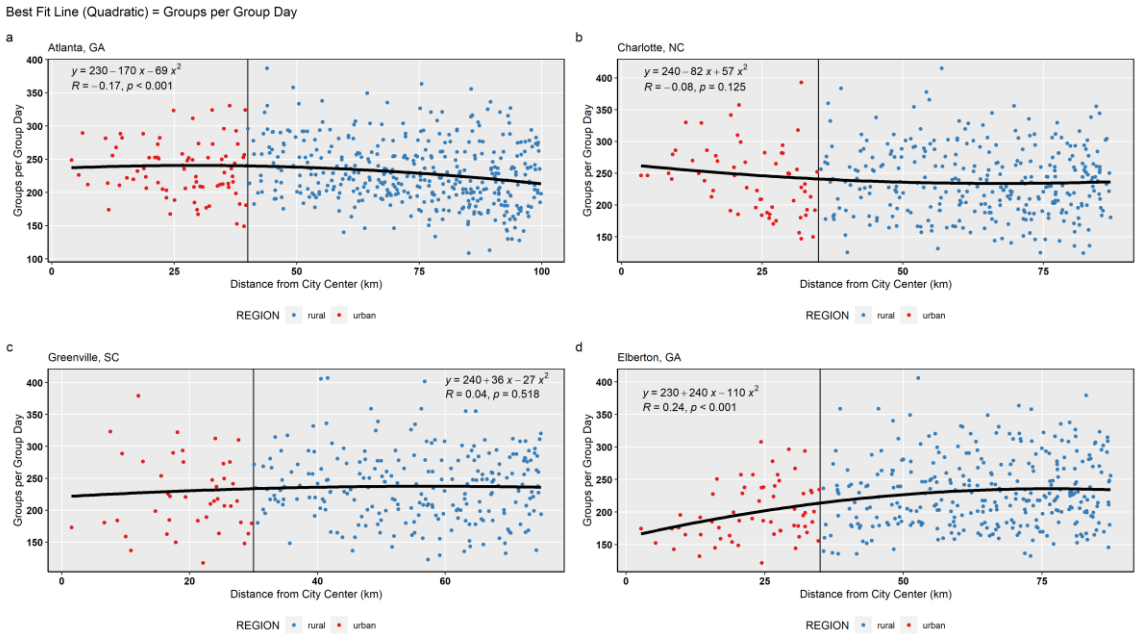

Figure 4.21: Scatterplots and quadratic line fits of mean warm season TL groups per group day versus distance from city center for the (**a**) Atlanta, (**b**) Charlotte, (**c**) Greenville, and (**d**) Elberton (control) domains over the 4-year study period (2018–2021).

4.2.2 Statistical analysis

Within the Atlanta domain, assessment of each CG flash metric's mean between urban versus rural distributions (displayed in Table 4.1) revealed increases of 22%, 7–8%, and 14% for CG flash count, flash days, and flashes per flash day, respectively. For TL group count, group days, and groups per group day, there were increases of 11–20%, 8%, and 3–12%, respectively, as shown in Table 4.2. Results from the independent samples *t* tests and Mann-Whitney *U* tests displayed in tables 4.3–4.6 found statistically significant ($\alpha = 0.05$) increases in the means of all metrics within Atlanta's urban core, except for TL groups per group day when assessed using the geometric urban buffer ($t = 1.08$, $p = .283$), rather than the NLCD-based delineation.

For the Charlotte domain, increases of 15–25% and 17–23% were calculated for CG flash count and flashes per flash day, while flash days ranged from a 1% decrease when using the geometric delineation to a 2% increase for the NLCD-based delineation. Similarly, hypothesis testing found statistically significant increases in CG flash count and flashes per flash day for both delineations, while no significant difference was found for flash days using either delineation. Results for the TL group metrics were more disparate between delineation methods. Using the primitive geometric buffers, Charlotte's group count and days displayed decreases of 5.8% and 7.8%, respectively, with a 1.9% increase in mean groups per group day. Using the NLCD-based delineation, mean group count and groups per group day increased by 5.9% and 9.9%, respectively, while group days decreased by 3.5%. The results of significance testing displayed a significant decrease in group days when using the geometric buffer ($t = -3.90$, $p < .001$), and a significant increase in groups per group day when using the NLCD-based delineation ($t = 1.98$, $p = .048$). This outcome is in line with the results of the visual and graphical analyses. It appears likely that Charlotte's NLCD-based urban delineation offers a

significant improvement over the primitive geometric buffer with regard to capturing those areas most strongly influenced by the urban core.

These results indicate that the urban forcing provided by Charlotte is largely supplementary to natural geophysical factors (e.g., orographic preferences) which act as the dominant controls on the distributions of lightning intensity and frequency. While Atlanta's spatially dense sprawl has displayed an ability to initiate thunderstorms that would not have otherwise occurred, Charlotte's smaller urban core likely precludes it from serving as a dominant forcing in thunderstorm initiation and resultant lightning production. Furthermore, though enhancement of TL group count and groups per group was observed, it is apparent that CG strike intensity is most significantly influenced by Charlotte's core. As mentioned by McLeod et al. (2017) and Miller et al. (2015), there is likely a complex interaction between terrain-related boundary layer processes (e.g., downslope circulations due to differential heating, orographic forcing for ascent, etc.) and urban-induced mesocirculations, among other factors, that deserves further investigation with improved methods and resources.

Greenville's urban delineations displayed increases in CG flash count, flash days, and flashes per flash day of 9–10%, 1–3%, and 7–8%, respectively, though the only statistically significant increase was found for flashes per flash day when utilizing the primitive geometric buffer. Conversely, TL metrics were notably lower within Greenville's urban delineations. The means of group count and groups per group day were 9–18% and 6–18% lower within the core, respectively, and both displayed statistically significant differences depending on the core sampling method used. Group days were 3.4% lower for the geometric delineation and 0.2% higher for the NLCD-based delineation. This exposes another limitation of the implemented methodology, as the coarse resolution of the lightning data and smaller scale of the Greenville

domain results in only four (eight) individual NLDN (GLM) cells being included in the NLCD-based urban delineation. Additionally, the inadequacy of the methodology is exacerbated by the orientation of the greater Greenville-Spartanburg area's urban sprawl.

Once again serving to validate the urban influences detected in the previous analyses, the mean CG flash count, flash days, and flashes per flash day within Elberton's surrogate urban sample were 18.1%, 8.9%, and 9.1% lower than in the surrounding rural sample, respectively. Furthermore, these differences were found to be statistically significant when assessed with the Student's *t* tests and Mann-Whitney *U* tests. Similarly, the surrogate urban sample experienced decreases of 15.4%, 1.9%, and 13.9% in TL group count, group days, and groups per group day, respectively. As anticipated following the visual analysis of Elberton's TL climatology, the only TL metric to display a statistically insignificant difference between the rural and surrogate urban buffer was TL group days (t = -1.53, p = .128).

Table 4.1: Percentage change in the mean of each CG flash metric between the urban and rural delineations of each Charlanta city (JJA, 2007–2021).

City (urban delineation)	Flash count	Flash days	Flashes per flash day
Atlanta (40 km buffer)	+21.9%	+7.3%	+14.0%
Atlanta (50% NLCD)	+22.2%	+8.2%	+13.7%
Greenville (30 km buffer)	+8.7%	+0.6%	+7.1%
Greenville (50% NLCD)	+10.0%	+2.5%	+7.7%
Charlotte (35 km buffer)	+15.3%	-0.9%	+16.9%
Charlotte (50% NLCD)	+24.6%	+2.3%	+23.0%
Elberton (35 km buffer)	-18.1%	-8.9%	-9.1%

Table 4.2: Percentage change in the mean of each TL group metric between the urban and rural delineations of each Charlanta city (JJA, 2018–2021).

City (urban delineation)	Group count	Group days	Groups per group day
Atlanta (40 km buffer)	+11.0%	+7.9%	+2.6%
Atlanta (50% NLCD)	+20.3%	+8.0%	+11.6%
Greenville (30 km buffer)	-9.1%	-3.4%	-5.6%
Greenville (50% NLCD)	-17.7%	+0.2%	-17.9%
Charlotte (35 km buffer)	-5.8%	-7.8%	+1.9%
Charlotte (50% NLCD)	+5.9%	-3.5%	+9.9%
Elberton (35 km buffer)	-15.4%	-1.9%	-13.1%

Table 4.3: Results from independent samples *t* tests ($\alpha = 0.05$) conducted to assess for significant difference between the mean of each CG flash metric (JJA, 2007–2021).

City (urban delineation)	Flash count		Flash days		Flashes per flash day	
	t	*p*	*t*	*p*	*t*	*p*
Atlanta (40 km buffer)	9.64	< .001	9.26	< .001	7.06	< .001
Atlanta (50% NLCD)	8.60	< .001	9.22	< .001	6.09	< .001
Greenville (30 km buffer)	1.94	.054	0.21	.835	2.26	.025
Greenville (50% NLCD)	0.91	.365	0.37	.714	0.99	.326
Charlotte (35 km buffer)	5.19	< .001	-0.82	.413	6.69	< .001
Charlotte (50% NLCD)	5.13	< .001	1.25	.212	5.48	< .001
Elberton (35 km buffer)	-4.98	< .001	-6.01	< .001	-3.23	.001

Table 4.4: Results from Mann-Whitney *U* tests (α = 0.05) conducted to assess for significant difference between the median of each CG flash metric (JJA, 2007–2021).

City (urban delineation)	**Flash count**		**Flash days**		**Flashes per flash day**	
	U	*p*	*U*	*p*	*U*	*p*
Atlanta (40 km buffer)	11556	< .001	11305	< .001	10553	< .001
Atlanta (50% NLCD)	9033	< .001	9260	< .001	8103	< .001
Greenville (30 km buffer)	2597	.040	2291	.411	2729	< .001
Greenville (50% NLCD)	445	.331	411	.524	447	.321
Charlotte (35 km buffer)	5454	< .001	3521	.629	5826	< .001
Charlotte (50% NLCD)	2361	< .001	1755	.113	2372	< .001
Elberton (35 km buffer)	1963	< .001	1605	< .001	2580	.001

Table 4.5: Results from independent samples *t* tests ($\alpha = 0.05$) conducted to assess for significant difference between the mean of each TL group metric (JJA, 2018–2021).

City (urban delineation)	**Group count**		**Group days**		**Groups per group day**	
	t	*p*	*t*	*p*	*t*	*p*
Atlanta (40 km buffer)	4.28	< .001	10.68	< .001	1.08	.283
Atlanta (50% NLCD)	7.23	< .001	9.44	< .001	4.22	< .001
Greenville (30 km buffer)	-2.22	.027	-1.73	.085	-1.47	.143
Greenville (50% NLCD)	-1.97	.050	0.05	.963	-2.15	.032
Charlotte (35 km buffer)	-1.55	.122	-3.90	< .001	0.60	.553
Charlotte (50% NLCD)	1.00	.319	-1.10	.272	1.98	.048
Elberton (35 km buffer)	-4.77	< .001	-1.53	.128	-4.16	< .001

Table 4.6: Results from Mann-Whitney *U* tests (α = 0.05) conducted to assess for significant difference between the median of each GLM group metric (JJA, 2018–2021).

City (urban delineation)	**Group count**		**Group days**		**Groups per group day**	
	U	*p*	*U*	*p*	*U*	*p*
Atlanta (40 km buffer)	21104	< .001	26847	< .001	17750	.202
Atlanta (50% NLCD)	19388	< .001	21306	< .001	16903	< .001
Greenville (30 km buffer)	3981	.023	4305	.106	4330	.117
Greenville (50% NLCD)	621	.039	1136	.835	568	.021
Charlotte (35 km buffer)	8203	.169	6786	.001	9605	.629
Charlotte (50% NLCD)	4476	.168	3781	.959	4828	.035
Elberton (35 km buffer)	5823	< .001	8274	.099	6383	< .001

4.2.3 ANOVA and Tukey's HSD

Assessing the differences in mean lightning intensity and frequency between the urban samples of the four domains included in the study, one-way ANOVA was performed for both detection datasets. As displayed in Figures 4.22–4.25 below, the results revealed a statistically significant ($\alpha = 0.05$) difference in mean values between the core samples of at least two cities for all metrics ($p < .001$, except for TL groups per group day, for which $p < .005$). This indicates there is significant inter-urban variability in CG and TL intensity and frequency across the Charlanta megaregion. The Tukey's HSD post-hoc tests found a statistically significant difference in the mean of every CG flash metric between all pairs of cities using both core delineation schemes, except for CG flash count between Atlanta and Charlotte and flash days between Greenville and Charlotte. Synthesizing these results, it is apparent that mean CG flash count and flashes per flash day were most intense within the urban cores of Atlanta and Charlotte, with Greenville experiencing significantly less of each. Furthermore, the differences in the means of each CG flash metric between Elberton's surrogate buffer and the three urban cores were found to be statistically significant, which lends more support to the conclusion that Charlanta's major metropolitan areas enhance proximal CG flash production.

For the TL metrics, Tukey's HSD tests found significant differences in mean TL group count for all pairs of cities using both delineation schemes, except between Charlotte and both Greenville and Elberton. Statistically significant differences were found in mean TL group days between all pairs, except for Greenville and Elberton. Finally, the Tukey's HSD results for mean TL groups per group day were the most variable between each delineation scheme. Using the geometric buffer, statistically significant differences in mean TL groups per group day were only found between the pairs of Elberton and both Atlanta and Charlotte. Using the NLCD-based

delineation, statistically significant differences in mean TL groups per group day were found between all pairs of cities, except for Atlanta and Charlotte. All *p* values for the ANOVA and Tukey's HSD tests are displayed in Figures 4.22–4.25. Many of the TL patterns observed in the previous analyses were further elucidated in these results. For example, the significant enhancement of TL intensity and frequency within Atlanta's urban core relative to the other three cities and negligible enhancement of TL frequency within Charlotte's core.

Most prominently, these results highlight the importance of size, density, and layout, among other key features and conditions, in shaping a city's potential to modify lightning production. This has been acknowledged in a number of previous studies (Changnon, 1992; Kingfield et al., 2018; Schmid and Niyogi, 2013; Westcott, 1995) and is further confirmed here. As expected, Atlanta's spatially dense and vast area of development displays the most significant urban signal in both CG and TL metrics, though it is again apparent that CG lightning distributions are most strongly influenced by the urban core.

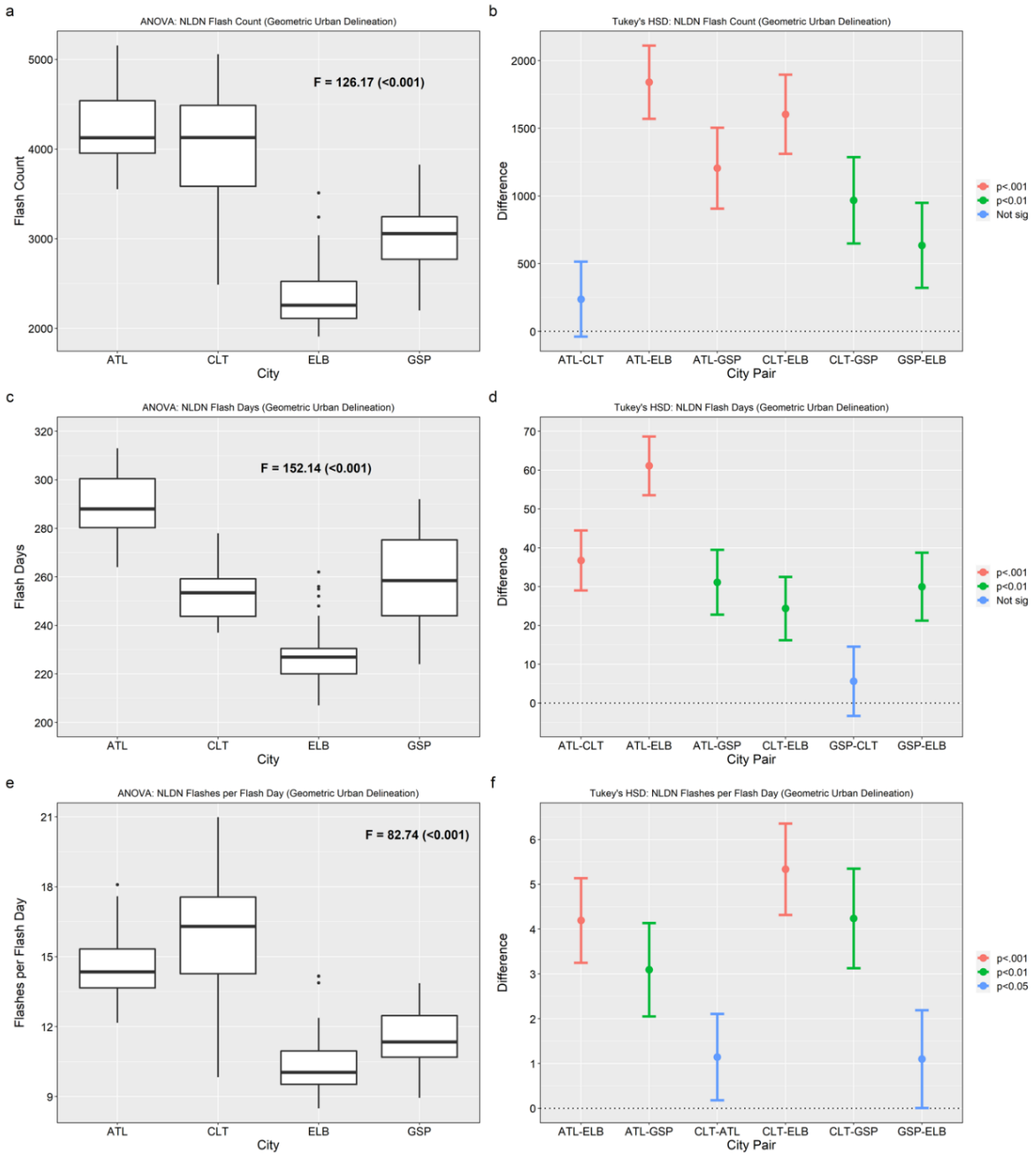

Figure 4.22: Differences in CG flash count (a), flash days (c), and flashes per flash day (e) between the geometric urban delineations of Charlanta's major cities. *F* values from the ANOVA tests reported along with their associated *p* values in parentheses. Results from the post-hoc tests for CG flash count (b), flash days (d), and flashes per flash day (f) are displayed at right.

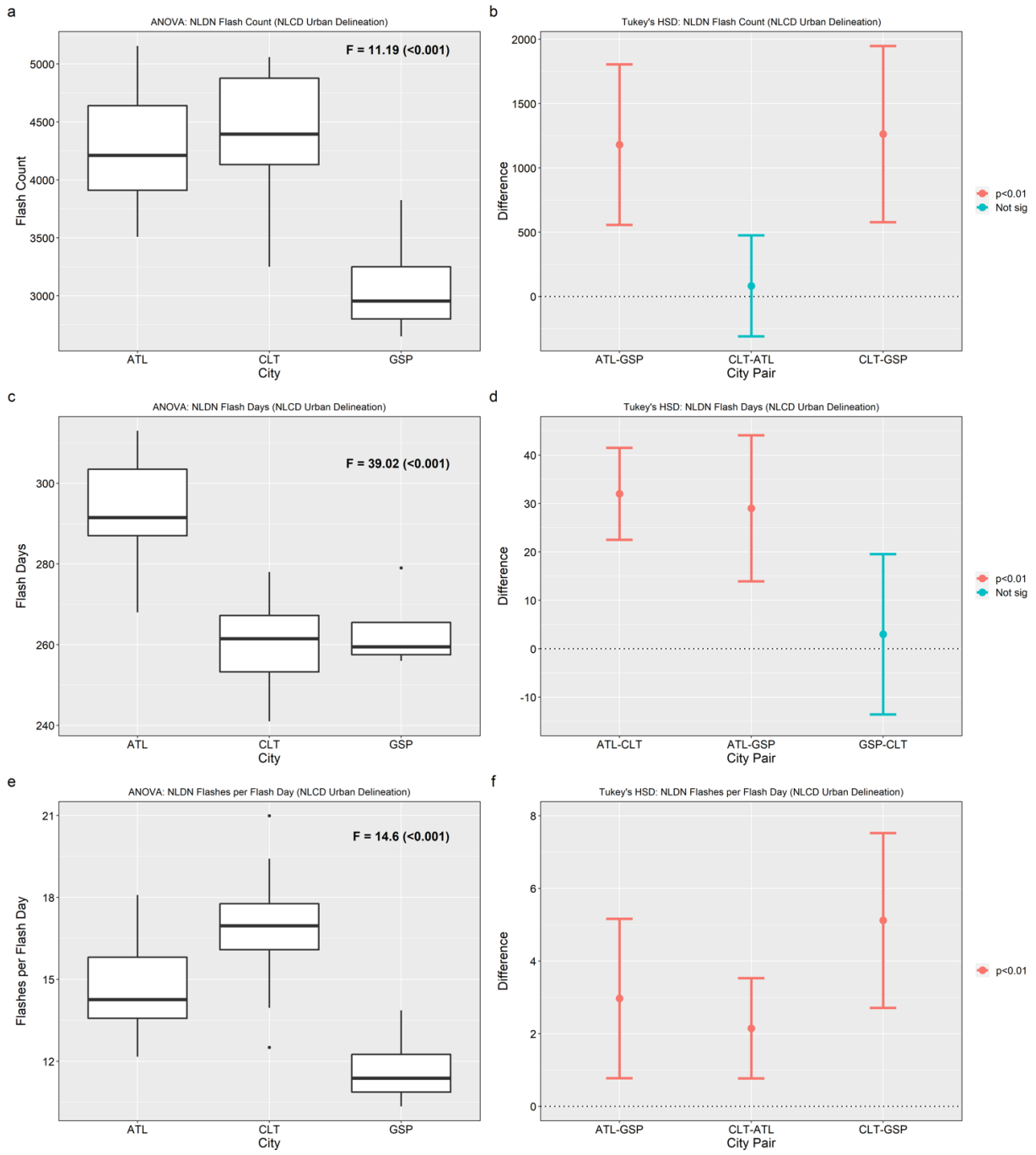

Figure 4.23: Differences in CG flash count (a), flash days (c), and flashes per flash day (e) between the NLCD urban delineations of Charlanta's major cities. *F* values from the ANOVA tests reported along with their associated *p* values in parentheses. Results from the post-hoc tests for CG flash count (b), flash days (d), and flashes per flash day (f) are displayed at right.

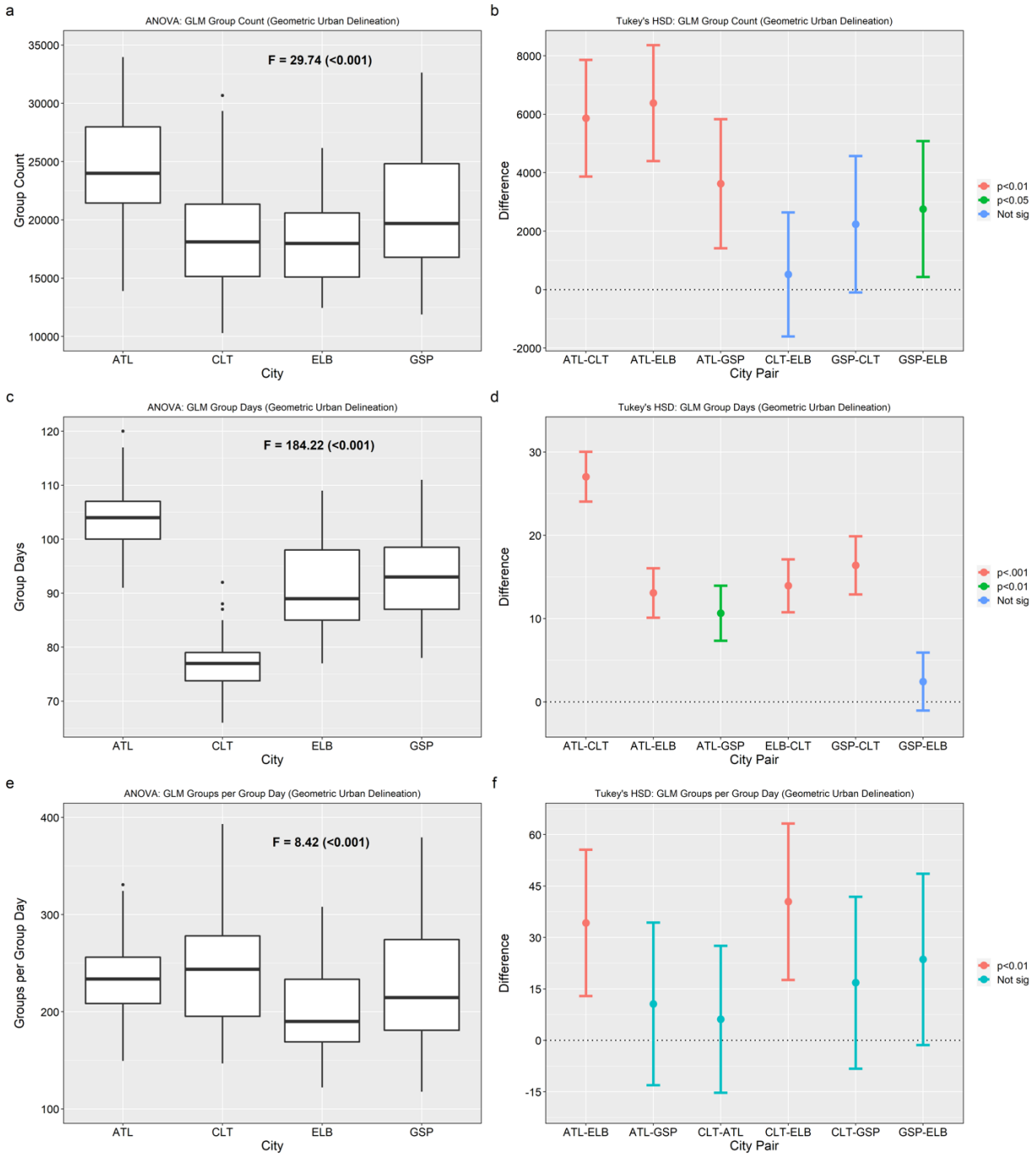

Figure 4.24: Differences in TL group count (a), group days (c), and groups per group day (e) between the geometric urban delineations of Charlanta's major cities. *F* values from the ANOVA tests reported with their associated *p* values in parentheses. Results from the post-hoc tests for TL group count (b), group days (d), and groups per group day (f) are displayed at right.

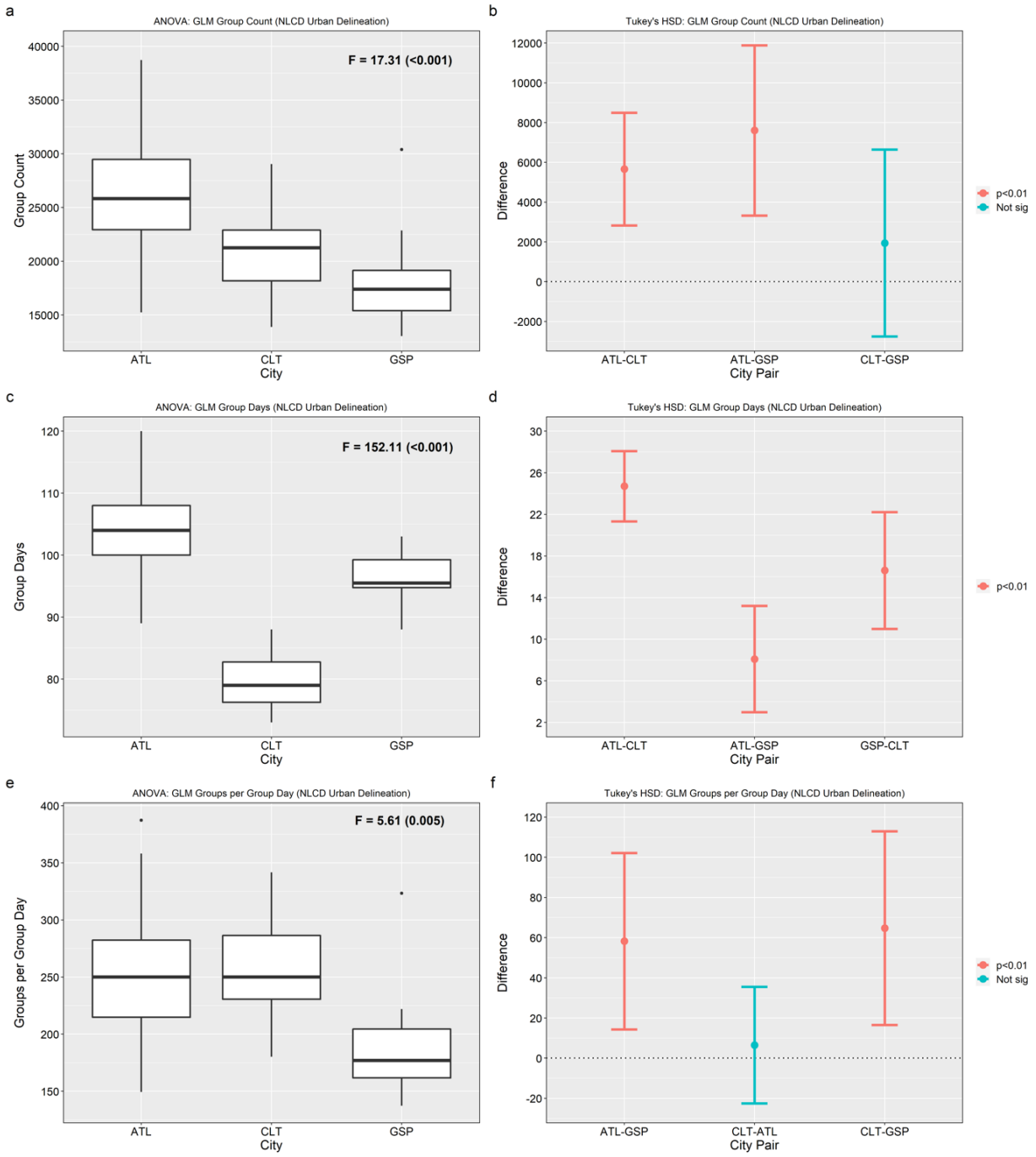

Figure 4.25 Differences in TL group count (a), group days (c), and groups per group day (e) between the NLCD urban delineations of Charlanta's major cities. *F* values from the ANOVA tests reported with their associated *p* values in parentheses. Results from the post-hoc tests for TL group count (b), group days (d), and groups per group day (f) are displayed at right.

CHAPTER 5

CONCLUSIONS

The Charlanta megaregion has been the focus of numerous investigations into urban influences on local atmospheric conditions and their signal in climatological trends (Debbage & Shepherd, 2018; Shepherd et al., 2013). As a rapidly expanding Urban Climate Archipelago (UCA), the continued monitoring of environmental conditions and hazards across the megaregion is of great importance for the millions of residents (Shepherd et al., 2014). Increasing spatial contiguity and accelerated expansion of urban sprawl are predicted to dramatically alter the spatial footprints of cities and megaregions, resulting in a widespread strengthening of the linkages between urban heat islands and their overlying boundary layer atmospheres (Debbage and Shepherd, 2015; Stone et al., 2013; Terando et al., 2014).

The principal objectives of this thesis were to construct an updated climatological synthesis of urban lightning enhancement at the novel spatial scale of the Charlanta megaregion, and to determine if an urban signal is resolvable in publicly available TL observations collected by the spaceborne GLM. Addressing research question #1, the applied methodological framework defined by Ashley et al. (2012) was modified to construct 15-year (2007-2021) warm season CG flash climatologies for Charlanta's constituent metropolitan areas and at the full megaregion-scale. Addressing research question #2, the aforementioned methodology was applied to the available temporal range (2018-2021) of provisionally mature GLM group data in order to investigate the influence of Charlanta's cities on TL intensity and frequency. As a result, this was the first study of the ULE to utilize data collected by the GLM, and therefore, the first to

utilize spatio-temporally continuous lightning observations from a satellite platform in geostationary orbit.

Many of the spatial patterns associated with the ULE noted in previous research were resolvable in the developed CG and TL climatologies, along with a set of new features hypothesized to be related to the spatio-temporal evolution of the ULE. Most prominently, significant enhancement of lightning intensity and frequency was apparent over and downwind of the larger cities in both forms of detection data, with a markedly diminished urban signal over the smaller city of Greenville. These observations echo the findings of Ashley et al. (2012) and a number of earlier studies (Huff and Changnon, 1973; Oke, 1982; Bentley et al., 2012) that urban morphological characteristics, namely, extent, density, and orientation, are key factors in determining the degree to which lightning occurrence is modified. Furthermore, in comparison with the results of Stallins and Bentley (2006) displayed in Figures 2.3 and 2.4, it is apparent that Atlanta's downwind anomaly between I-85 and I-20 may be expanding eastward and intensifying as the city's spatial characteristics evolve, though further investigation is certainly required to make such a conclusion. Finally, the results of this thesis underscore the importance of utilizing GLM TL data in future investigations of the ULE, while also highlighting the need for fundamental methodological improvements and the development of more sophisticated approaches to analyzing the ULE.

5.1 Thoughts on methodological improvements

There are several ways in which the implemented workflow could be improved with regard to data source characteristics, preparation of the lightning data before analysis, and methods of investigating the ULE, among many others. Among other findings, the topographical influences observed in the domains of Greenville and Charlotte highlight the need to use more innovative methodologies (e.g., Forney et al. (2022)) and stress the relatively coarse grid resolutions of the utilized lightning datasets. These small-scale features demand CG flash detection data gridded at a higher spatial resolution in order to adequately resolve the finer scale processes shaping the distributions of lightning intensity and frequency. In their comprehensive review of urban lightning research, Stallins and Rose (2008) emphasized the importance of bin size (i.e., grid cell resolution) and discussed several ULE studies performed at resolutions of 5 km or less (Ashley et al., 2012; Rose et al., 2008; Stallins and Bentley, 2006). Though this thesis prioritized using freely available sources of lightning observations, the use of commercial data, such as Vaisala's complete NLDN flash product, would allow for more adequate grid spacing. Another shortcoming of the implemented workflow was the lack of consideration for variability in NLDN performance characteristics, namely, CG flash detection efficiency, due to updates in the network's hardware and downstream algorithmic processing of the raw observations. This likely introduced spatio-temporal disparities in the detection data, resulting in lightning climatologies biased towards more recent years. Nevertheless, as with the issue of coarse grid cell resolution, the use of freely available NLDN observations limited the capacity to which such a consideration could be made.

Focusing on more easily rectifiable deficiencies, the threshold of at least one flash occurrence used to derive the number of flash days was likely susceptible to misclassification

due to errant observations (Hayward et al., 2020). Though it is unlikely to have had a significant impact on the analyses conducted, adjusting the threshold would bolster the integrity of the flash days metric. A more impactful deficiency of the employed methodology was the lack of an intensive effort to isolate lightning observations from days with absent synoptic forcing, only temporally filtering the datasets to the warm season months of June, July, and August. While this primitive scheme was deemed sufficient as weak ambient flow conditions generally dominate across the study area during these summer months, it is apparent that a more comprehensive approach could have been taken to prevent any contamination by observations collected during synoptically active conditions. An example of such an approach that has been successfully implemented in relevant work is the use of the Spatial Synoptic Classification (SSC) database to classify daily lightning observations by ambient air mass type (Kalkstein et al., 1996; Sheridan, 2002). The observations could then be filtered to include only those days with air mass classifications of Moist Tropical (MT), Moist Tropical Plus (MT+), or Moist Tropical Plus-Plus (MT++). As noted by Haberlie et al. (2015), these classifications practically characterize the conditionally unstable atmosphere known to be most strongly influenced by urban effects. Additionally, the UHI-induced air temperature gradient between cities and their rural surroundings (i.e., BLHI) is most pronounced on such days. Therefore, implementation of this procedure would allow for a more accurate assessment of the urban signal embedded within long-term lightning distributions.

REFERENCES

A bolt from the blue: What is lightning? - Social Media Blog - Bureau of Meteorology. (2019). [Blog]. Australian Bureau of Meteorology. https://media.bom.gov.au/social/blog/1478/a-bolt-from-the-blue-what-is-lightning/

ArcGIS Pro (2.9). (2021). Esri. https://pro.arcgis.com/en/pro-app/latest/tool-reference/main/arcgis-pro-tool-reference.htm

Ashley, W. S., Bentley, M. L., & Stallins, J. A. (2012). Urban-induced thunderstorm modification in the Southeast United States. *Climatic Change*, *113*(2), 481–498. https://doi.org/10.1007/s10584-011-0324-1

Baik, J., Kim, Y.-H., Kim, J.-J., & Han, J.-Y. (2007). Effects of boundary-layer stability on urban heat island-induced circulation. *Theoretical and Applied Climatology*, *89*, 73–81. https://doi.org/10.1007/s00704-006-0254-4

Bateman, M., Mach, D., & Stock, M. (2021). Further Investigation Into Detection Efficiency and False Alarm Rate for the Geostationary Lightning Mappers Aboard GOES-16 and GOES-17. *Earth and Space Science*, *8*(2), e2020EA001237. https://doi.org/10.1029/2020EA001237

Bell, T. L., Rosenfeld, D., & Kim, K.-M. (2009). Weekly cycle of lightning: Evidence of storm invigoration by pollution. *Geophysical Research Letters*, *36*(23). https://doi.org/10.1029/2009GL040915

Bentley, M. L., Ashley, W. S., & Stallins, J. A. (2011). Radar identification of urban-enhanced thunderstorm activity for Atlanta, Georgia, USA. *2011 Joint Urban Remote Sensing Event*, 413–416. https://doi.org/10.1109/JURSE.2011.5764807

Bentley, M. L., Sae-Jung, J., Kaminski, S., & Terry, C. C. (2021). A spatiotemporal analysis of lightning in the Bangkok Metropolitan Region. *Asian Geographer*, *0*(0), 1–22. https://doi.org/10.1080/10225706.2021.2010579

Bentley, M., Stallins, J., & Ashley, W. (2012). Synoptic environments favourable for urban convection in Atlanta, Georgia. *International Journal of Climatology*, *32*. https://doi.org/10.1002/joc.2344

Blakeslee, R. J., & Goodman, S. J. (1992). *Lightning Imaging Sensor (US) for the Earth Observing System*. 44.

Blaylock, B. K., & Horel, J. D. (2020). Comparison of Lightning Forecasts from the High-Resolution Rapid Refresh Model to Geostationary Lightning Mapper Observations. *Weather and Forecasting*, *35*(2), 401–416. https://doi.org/10.1175/WAF-D-19-0141.1

Boccippio, D. J., Koshak, W., Blakeslee, R., Driscoll, K., Mach, D., Buechler, D., Boeck, W., Christian, H. J., & Goodman, S. J. (2000). The Optical Transient Detector (OTD): Instrument Characteristics and Cross-Sensor Validation. *Journal of Atmospheric and Oceanic Technology*, *17*(4), 441–458. https://doi.org/10.1175/1520-0426(2000)017<0441:TOTDOI>2.0.CO;2

Boccippio, D. J., Koshak, W. J., & Blakeslee, R. J. (2002). Performance Assessment of the Optical Transient Detector and Lightning Imaging Sensor. Part I: Predicted Diurnal

Variability. *Journal of Atmospheric and Oceanic Technology*, *19*(9), 1318–1332. https://doi.org/10.1175/1520-0426(2002)019<1318:PAOTOT>2.0.CO;2

Bornstein, R., & Lin, Q. (2000). Urban heat islands and summertime convective thunderstorms in Atlanta: Three case studies. *Atmospheric Environment*, *34*(3), 507–516. https://doi.org/10.1016/S1352-2310(99)00374-X

Bürgesser, R. E. (2017). Assessment of the World Wide Lightning Location Network (WWLLN) detection efficiency by comparison to the Lightning Imaging Sensor (LIS). *Quarterly Journal of the Royal Meteorological Society*, *143*(708), 2809–2817. https://doi.org/10.1002/qj.3129

Carter, M., Shepherd, J. M., Burian, S., & Jeyachandran, I. (2012). *Integration of Lidar Data into a Coupled Mesoscale–Land Surface Model: A Theoretical Assessment of Sensitivity of Urban–Coastal Mesoscale Circulations to Urban Canopy Parameters in: Journal of Atmospheric and Oceanic Technology Volume 29 Issue 3 (2012).* https://journals.ametsoc.org/view/journals/atot/29/3/2011jtecha1524_1.xml

CPTEC. (2022). *Accumulated GOES-16 GLM Data.* http://ftp.cptec.inpe.br/goes/goes16/goes16_web/glm_acumulado_nc/

Changnon, S. A. (1992). Inadvertent Weather Modification in Urban Areas: Lessons for Global Climate Change. *Bulletin of the American Meteorological Society*, *73*(5), 619–627. https://doi.org/10.1175/1520-0477(1992)073<0619:IWMIUA>2.0.CO;2

Changnon, S. A., Huff, F. A., & Semonin, R. G. (1971). METROMEX: An investigation of inadvertent weather modification. *Bulletin of the American Meteorological Society*, *52*(10), 958–968. https://doi.org/10.1175/1520-0477(1971)052<0958:MAIOIW>2.0.CO;2

Chen, F., & Miao, S. (2008). Formation of horizontal convective rolls in urban area. *Atmos*, *89*, 298–304.

Cintineo, J. L., Pavolonis, M. J., & Sieglaff, J. M. (2022). ProbSevere LightningCast: A Deep-Learning Model for Satellite-Based Lightning Nowcasting. *Weather and Forecasting*, *37*(7), 1239–1257. https://doi.org/10.1175/WAF-D-22-0019.1

Cummins, K. L., & Murphy, M. J. (2009). An Overview of Lightning Locating Systems: History, Techniques, and Data Uses, With an In-Depth Look at the U.S. NLDN. *IEEE Transactions on Electromagnetic Compatibility*, *51*(3), 499–518. https://doi.org/10.1109/TEMC.2009.2023450

Danielson, J. J., & Gesch, D. B. (2011). *Global multi-resolution terrain elevation data 2010 (GMTED2010)* (Report No. 2011–1073; Open-File Report). USGS Publications Warehouse. https://doi.org/10.3133/ofr20111073

Debbage, N. (2019). Multiscalar spatial analysis of urban flood risk and environmental justice in the Charlanta megaregion, USA. *Anthropocene*, *28*, 100226. https://doi.org/10.1016/j.ancene.2019.100226

Debbage, N., McLeod, J., Rackley, J., Zhu, L., Mote, T. L., & Grundstein, A. J. (2015). The Influence of Point Source Aerosol Emissions on Atmospheric Convective Activity in the Vicinity of Power Plants in Georgia, USA. *Papers in Applied Geography*, *1*(2), 134–142. https://doi.org/10.1080/23754931.2015.1012430

Debbage, N., & Shepherd, J. M. (2015). The urban heat island effect and city contiguity. *Computers, Environment and Urban Systems*, *54*, 181–194. https://doi.org/10.1016/j.compenvurbsys.2015.08.002

Debbage, N., & Shepherd, M. (2018). The Influence of Urban Development Patterns on Streamflow Characteristics in the Charlanta Megaregion. *Water Resources Research, 54*. https://doi.org/10.1029/2017WR021594

Diem, J. E. (2008). Detecting summer rainfall enhancement within metropolitan Atlanta, Georgia USA. *International Journal of Climatology*, *28*(1), 129–133. https://doi.org/10.1002/joc.1560

Diem, J. E., & Mote, T. L. (2005). Interepochal Changes in Summer Precipitation in the Southeastern United States: Evidence of Possible Urban Effects near Atlanta, Georgia. *Journal of Applied Meteorology and Climatology*, *44*(5), 717–730. https://doi.org/10.1175/JAM2221.1

Diffenbaugh, N. S., Scherer, M., & Trapp, R. J. (2013). Robust increases in severe thunderstorm environments in response to greenhouse forcing. *Proceedings of the National Academy of Sciences*, *110*(41), 16361–16366. https://doi.org/10.1073/pnas.1307758110

Dixon, P. G., & Mote, T. L. (2003). Patterns and Causes of Atlanta's Urban Heat Island–Initiated Precipitation. *Journal of Applied Meteorology and Climatology*, *42*(9), 1273–1284. https://doi.org/10.1175/1520-0450(2003)042<1273:PACOAU>2.0.CO;2

Fairman, S. I., & Bitzer, P. M. (2022). The Detection of Continuing Current in Lightning Using the Geostationary Lightning Mapper. *Journal of Geophysical Research: Atmospheres*, *127*(5), e2020JD033451. https://doi.org/10.1029/2020JD033451

Fan, J., Zhang, Y., Li, Z., Hu, J., & Rosenfeld, D. (2020). Urbanization-induced land and aerosol impacts on sea-breeze circulation and convective precipitation. *Atmospheric Chemistry and Physics*, *20*(22), 14163–14182. https://doi.org/10.5194/acp-20-14163-2020

Forney, R. K., Debbage, N., Miller, P., & Uzquiano, J. (2022). Urban effects on weakly forced thunderstorms observed in the Southeast United States. *Urban Climate*, *43*, 101161. https://doi.org/10.1016/j.uclim.2022.101161

Goodman, S. J., Blakeslee, R. J., Koshak, W. J., Mach, D., Bailey, J., Buechler, D., Carey, L., Schultz, C., Bateman, M., McCaul, E., & Stano, G. (2013). The GOES-R Geostationary Lightning Mapper (GLM). *Atmospheric Research*, *125–126*, 34–49. https://doi.org/10.1016/j.atmosres.2013.01.006

Goodman, S., Mach, D., Koshak, W., & Blakeslee, R. (2012). *GLM Lightning Cluster-Filter Algorithm*. 73.

Gupta, P., Remer, L. A., Patadia, F., Levy, R. C., & Christopher, S. A. (2020). High-Resolution Gridded Level 3 Aerosol Optical Depth Data from MODIS. *Remote Sensing*, *12*(17), Article 17. https://doi.org/10.3390/rs12172847

Haberlie, A. M., Ashley, W. S., Fultz, A. J., & Eagan, S. M. (2016). The effect of reservoirs on the climatology of warm-season thunderstorms in Southeast Texas, USA: RESERVOIRS AND THUNDERSTORMS. *International Journal of Climatology*, *36*(4), 1808–1820. https://doi.org/10.1002/joc.4461

Haberlie, A. M., Ashley, W. S., & Pingel, T. J. (2015). The effect of urbanisation on the climatology of thunderstorm initiation. *Quarterly Journal of the Royal Meteorological Society*, *141*(688), 663–675. https://doi.org/10.1002/qj.2499

Han, J.-Y., & Baik, J.-J. (2008). A Theoretical and Numerical Study of Urban Heat Island–Induced Circulation and Convection. *Journal of the Atmospheric Sciences*, *65*(6), 1859–1877. https://doi.org/10.1175/2007JAS2326.1

Harlan, S. L., Brazel, A. J., Darrel, J. G., Jones, N. S., Larsen, L., Prashad, L., & Stefanov, W. L. (2007). In the shade of affluence: The inequitable distribution of the urban heat island. In R. C. Wilkinson & W. R. Freudenburg (Eds.), *Equity and the Environment* (Vol. 15, pp. 173–202). Emerald Group Publishing Limited. https://doi.org/10.1016/S0196-1152(07)15005-5

Hayward, L., Whitworth, M., Pepin, N., & Dorling, S. (2020). Review article: A comprehensive review of datasets and methodologies employed to produce thunderstorm climatologies. *Natural Hazards and Earth System Sciences*, *20*(9), 2463–2482. https://doi.org/10.5194/nhess-20-2463-2020

Heever, S. C. van den, & Cotton, W. R. (2007). Urban Aerosol Impacts on Downwind Convective Storms. *Journal of Applied Meteorology and Climatology*, *46*(6), 828–850. https://doi.org/10.1175/JAM2492.1

Heisler, G., & Brazel, A. (2010). The urban physical environment: Temperature and urban heat islands. *Urban Ecosystem Ecology*, 29–56.

Hersbach, H., Bell, B., Berrisford, P., Hirahara, S., Horányi, A., Muñoz-Sabater, J., Nicolas, J., Peubey, C., Radu, R., Schepers, D., Simmons, A., Soci, C., Abdalla, S., Abellan, X., Balsamo, G., Bechtold, P., Biavati, G., Bidlot, J., Bonavita, M., … Thépaut, J.-N. (2020). The ERA5 global reanalysis. *Quarterly Journal of the Royal Meteorological Society*, *146*(730), 1999–2049. https://doi.org/10.1002/qj.3803

Heuscher, L., Liu, C., Gatlin, P., & Petersen, W. A. (2022). Relationship Between Lightning, Precipitation, and Environmental Characteristics at Mid-/High Latitudes From a GLM and GPM Perspective. *Journal of Geophysical Research: Atmospheres*, *127*(13), e2022JD036894. https://doi.org/10.1029/2022JD036894

Hidalgo, J., Masson, V., Baklanov, A., Pigeon, G., & Gimeno, L. (2008). Advances in Urban Climate Modeling. Trends and Directions in Climate Research. *Annals of the New York Academy of Sciences, 1146*, 354–374.

Higuchi, A. (2021). Toward More Integrated Utilizations of Geostationary Satellite Data for Disaster Management and Risk Mitigation. *Remote Sensing*, *13*(8), Article 8. https://doi.org/10.3390/rs13081553

Huff, F. A., & Changnon, S. A. (1973). Precipitation modification by major urban areas. *Bulletin of the American Meteorological Society*, *54*(12), 1220–1233. https://doi.org/10.1175/1520-0477(1973)054<1220:PMBMUA>2.0.CO;2

Jin, M., Shepherd, M., & King, M. (2005). Urban aerosols and their variations with clouds and rainfall: A case study for New York and Houston. *J. Geophys. Res*, *110*. https://doi.org/10.1029/2004JD005081

Johnson, B. D., Williams, M. D., & Shepherd, J. M. (2021). Urbanization and Winter Precipitation: A Case Study Analysis of Land Surface Sensitivity. *Atmosphere*, *12*(7), Article 7. https://doi.org/10.3390/atmos12070805

Kalashnikov, D. A., Loikith, P. C., Catalano, A. J., Waliser, D. E., Lee, H., & Abatzoglou, J. T. (2020). A 30-Yr Climatology of Meteorological Conditions Associated with Lightning Days in the Interior Western United States. *Journal of Climate*, *33*(9), 3771–3785. https://doi.org/10.1175/JCLI-D-19-0564.1

Kalkstein, L. S., Nichols, M. C., Barthel, C. D., & Greene, J. S. (1996). A New Spatial Synoptic Classification: Application to Air-Mass Analysis. *International Journal of Climatology*,

16(9), 983–1004. https://doi.org/10.1002/(SICI)1097-0088(199609)16:9<983::AID-JOC61>3.0.CO;2-N

Kaplan, J. O., & Lau, K. H.-K. (2021). The WGLC global gridded lightning climatology and time series. *Earth System Science Data*, *13*(7), 3219–3237. https://doi.org/10.5194/essd-13-3219-2021

Kar, S. K., Liou, Y.-A., & Ha, K.-J. (2007). Characteristics of cloud-to-ground lightning activity over Seoul, South Korea in relation to an urban effect. *Annales Geophysicae*, *25*(10), 2113–2118. https://doi.org/10.5194/angeo-25-2113-2007

Kato, S., & Yamaguchi, Y. (2007). Estimation of storage heat flux in an urban area using ASTER data. *Remote Sensing of Environment*, *110*(1), 1–17. https://doi.org/10.1016/j.rse.2007.02.011

Katona, B., Markowski, P., Alexander, C., & Benjamin, S. (2016). The Influence of Topography on Convective Storm Environments in the Eastern United States as Deduced from the HRRR. *Weather and Forecasting*, *31*(5), 1481–1490. https://doi.org/10.1175/WAF-D-16-0038.1

Kaufmann, J., & Schering, A. (2014). Analysis of Variance ANOVA. In *Wiley StatsRef: Statistics Reference Online*. John Wiley & Sons, Ltd. https://doi.org/10.1002/9781118445112.stat06938

Kingfield, D. M., Calhoun, K. M., Beurs, K. M. de, & Henebry, G. M. (2018). Effects of City Size on Thunderstorm Evolution Revealed through a Multiradar Climatology of the Central United States. *Journal of Applied Meteorology and Climatology*, *57*(2), 295–317. https://doi.org/10.1175/JAMC-D-16-0341.1

Koshak, W. J., Cummins, K. L., Buechler, D. E., Vant-Hull, B., Blakeslee, R. J., Williams, E. R., & Peterson, H. S. (2015). Variability of CONUS Lightning in 2003–12 and Associated Impacts. *Journal of Applied Meteorology and Climatology*, *54*(1), 15–41. https://doi.org/10.1175/JAMC-D-14-0072.1

Koshak, W., Mach, D., Bateman, M., Armstrong, P., & Virts, K. (2018). *Product Performance Guide For Data Users*. 16.

Lay, E., Rodger, C., Holzworth, R., & Dowden, R. (2005). *Introduction to the World Wide Lightning Location Network (WWLLN)*.

Liu, J., & Niyogi, D. (2019). Meta-analysis of urbanization impact on rainfall modification. *Scientific Reports*, *9*(1), 7301. https://doi.org/10.1038/s41598-019-42494-2

Lopez, P. (2020). *Quality Control for GOES Geostationary Lightning Mapper Level-2 flash products*. ECMWF. https://doi.org/10.21957/micszfbkq

Losos, D., Pitts, K., & McHugh, M. (2020). *Accessing GOES-R series data from cloud platforms to create a value-added tool for end users*. *11501*. https://doi.org/10.1117/12.2568677

Lowry, W. P. (1998). Urban effects on precipitation amount. *Progress in Physical Geography: Earth and Environment*, *22*(4), 477–520. https://doi.org/10.1177/030913339802200403

Macgorman, D., Burgess, D., Mazur, V., Rust, W., & Taylor, W. (1989). Lightning Rates Relative to Tornadic Storm Evolution on 22 May 1981. *Journal of the Atmospheric Sciences*, *46*. https://doi.org/10.1175/1520-0469(1989)046<0221:LRRTTS>2.0.CO;2

MacGorman, D. R., Apostolakopoulos, I. R., Lund, N. R., Demetriades, N. W. S., Murphy, M. J., & Krehbiel, P. R. (2011). The Timing of Cloud-to-Ground Lightning Relative to Total

Lightning Activity. *Monthly Weather Review*, *139*(12), 3871–3886. https://doi.org/10.1175/MWR-D-11-00047.1

MacGorman, D. R., & Rust, W. D. (1998). *The Electrical Nature of Storms*. Oxford University Press.

MacGorman, D. R., & Taylor, W. L. (1989). Positive cloud-to-ground lightning detection by a direction-finder network. *Journal of Geophysical Research: Atmospheres*, *94*(D11), 13313–13318. https://doi.org/10.1029/JD094iD11p13313

Mann, H. B., & Whitney, D. R. (1947). On a Test of Whether one of Two Random Variables is Stochastically Larger than the Other. *The Annals of Mathematical Statistics*, *18*(1), 50–60. https://doi.org/10.1214/aoms/1177730491

Marchand, M., Hilburn, K., & Miller, S. D. (2019). Geostationary Lightning Mapper and Earth Networks Lightning Detection Over the Contiguous United States and Dependence on Flash Characteristics. *Journal of Geophysical Research: Atmospheres*, *124*(21), 11552–11567. https://doi.org/10.1029/2019JD031039

Mashhoodi, B. (2021). Environmental justice and surface temperature: Income, ethnic, gender, and age inequalities. *Sustainable Cities and Society*, *68*, 102810. https://doi.org/10.1016/j.scs.2021.102810

McLeod, J., & Shepherd, J.M. (2022). A Synoptic Framework for Forecasting the Urban Rainfall Effect Using Composite and K-Means Cluster Analyses. *Frontiers in Environmental Science*, *10*. https://www.frontiersin.org/article/10.3389/fenvs.2022.808026

McLeod, J., Shepherd, M., & Konrad, C. E. (2017). Spatio-temporal rainfall patterns around Atlanta, Georgia and possible relationships to urban land cover. *Urban Climate*, *21*, 27–42. https://doi.org/10.1016/j.uclim.2017.03.004

McNitt, J., Mozer, K., McNamara, D., & Martin, G. (2020). Chapter 22—GOES-R Series Data Access and Dissemination. In S. J. Goodman, T. J. Schmit, J. Daniels, & R. J. Redmon (Eds.), *The GOES-R Series* (pp. 261–271). Elsevier. https://doi.org/10.1016/B978-0-12-814327-8.00022-6

Medici, G., Cummins, K. L., Cecil, D. J., Koshak, W. J., & Rudlosky, S. D. (2017). The Intracloud Lightning Fraction in the Contiguous United States. *Monthly Weather Review*, *145*(11), 4481–4499. https://doi.org/10.1175/MWR-D-16-0426.1

Metropolitan and Micropolitan Statistical Areas Population Totals and Components of Change: 2010-2019. (n.d.). US Census Bureau. Retrieved October 24, 2021, from https://www.census.gov/data/tables/time-series/demo/popest/2010s-total-metro-and-micro-statistical-areas.html

Mialdea-Flor, I., Segura-Garcia, J., Felici-Castell, S., Garcia-Pineda, M., Alcaraz-Calero, J. M., & Navarro-Camba, E. (2019). Development of a Low-Cost IoT System for Lightning Strike Detection and Location. *Electronics, 8*(12), 1512. https://doi.org/10.3390/electronics8121512

Miller, P., Ellis, A. W., & Keighton, S. (2015). Spatial distribution of lightning associated with low-shear thunderstorm environments in the central Appalachian region. *Physical Geography*, *36*(2), 127–141. https://doi.org/10.1080/02723646.2015.1011257

Miller, P. W., & Mote, T. L. (2017a). Standardizing the Definition of a “Pulse” Thunderstorm. *Bulletin of the American Meteorological Society*, *98*(5), 905–913. https://doi.org/10.1175/BAMS-D-16-0064.1

Miller, P. W., & Mote, T. L. (2017b). A Climatology of Weakly Forced and Pulse Thunderstorms in the Southeast United States. *Journal of Applied Meteorology and Climatology*, *56*(11), 3017–3033. https://doi.org/10.1175/JAMC-D-17-0005.1

Mohajerani, A., Bakaric, J., & Jeffrey-Bailey, T. (2017). The urban heat island effect, its causes, and mitigation, with reference to the thermal properties of asphalt concrete. *Journal of Environmental Management*, *197*, 522–538. https://doi.org/10.1016/j.jenvman.2017.03.095

Mote, T. L., Lacke, M. C., & Shepherd, J. M. (2007). Radar signatures of the urban effect on precipitation distribution: A case study for Atlanta, Georgia. *Geophysical Research Letters*, *34*(20). https://doi.org/10.1029/2007GL031903

Murphy, M. J., Cramer, J. A., & Said, R. K. (2021). Recent History of Upgrades to the U.S. National Lightning Detection Network. *Journal of Atmospheric and Oceanic Technology*, *38*(3), 573–585. https://doi.org/10.1175/JTECH-D-19-0215.1

Murphy, M. S., & Konrad, C. E. (2005). Spatial and Temporal Patterns of Thunderstorm Events that Produce Cloud-to-Ground Lightning in the Interior Southeastern United States. *Monthly Weather Review*, *133*(6), 1417–1430. https://doi.org/10.1175/MWR2924.1

Naccarato, K. P., Pinto Jr., O., & Pinto, I. R. C. A. (2003). Evidence of thermal and aerosol effects on the cloud-to-ground lightning density and polarity over large urban areas of Southeastern Brazil. *Geophysical Research Letters*, *30*(13). https://doi.org/10.1029/2003GL017496

Nag, A., Murphy, M. J., Cummins, K. L., Pifer, A. E., & Cramer, J. A. (2014). *Recent Evolution of the U.S. National Lightning Detection Network*. 6.

Naylor, J., & Kennedy, A. (2021). Variability in Isolated Convective Activity between Louisville, Kentucky, and Nearby Rural Locations. *Earth Interactions*, *25*, 33–45. https://doi.org/10.1175/EI-D-20-0012.1

Ntelekos, A. A., Smith, J. A., Baeck, M. L., Krajewski, W. F., Miller, A. J., & Goska, R. (2008). Extreme hydrometeorological events and the urban environment: Dissecting the 7 July 2004 thunderstorm over the Baltimore MD Metropolitan Region. *Water Resources Research*, *44*(8). https://doi.org/10.1029/2007WR006346

Oda, P. S. S., Enoré, D. P., Mattos, E. V., Gonçalves, W. A., & Albrecht, R. I. (2022). An initial assessment of the distribution of total Flash Rate Density (FRD) in Brazil from GOES-16 Geostationary Lightning Mapper (GLM) observations. *Atmospheric Research*, *270*, 106081. https://doi.org/10.1016/j.atmosres.2022.106081

Oke, T. R. (1982). The energetic basis of the urban heat island. *Quarterly Journal of the Royal Meteorological Society*, *108*(455), 1–24. https://doi.org/10.1002/qj.49710845502

Oke, T. R. (1988). The urban energy balance. *Progress in Physical Geography: Earth and Environment*, *12*(4), 471–508. https://doi.org/10.1177/030913338801200401

Oke, T. R., & Cleugh, H. A. (1987). Urban heat storage derived as energy balance residuals. *Boundary-Layer Meteorology*, *39*(3), 233–245. https://doi.org/10.1007/BF00116120

Orville, R. (2008). Development of the National Lightning Detection Network. *Bulletin of The American Meteorological Society - BULL AMER METEOROL SOC*, *89*. https://doi.org/10.1175/BAMS-89-2-180

Orville, R. E., Henderson, R. W., & Bosart, L. F. (1983). An East Coast Lightning Detection Network. *Bulletin of the American Meteorological Society*, *64*(9), 1029–1037. https://doi.org/10.1175/1520-0477(1983)064<1029:AECLDN>2.0.CO;2

Orville, R. E., Huffines, G., Nielsen-Gammon, J., Zhang, R., Ely, B., Steiger, S., Phillips, S., Allen, S., & Read, W. (2001). Enhancement of cloud-to-ground lightning over Houston, Texas. *Geophysical Research Letters*, *28*(13), 2597–2600. https://doi.org/10.1029/2001GL012990

Patrinos, A. A., Chen, N. C. J., & Miller, R. L. (1978). *Precipitation studies around Plant Bowen*.

Peterson, M. (2019). Research Applications for the Geostationary Lightning Mapper Operational Lightning Flash Data Product. *Journal of Geophysical Research: Atmospheres*, *124*(17–18), 10205–10231. https://doi.org/10.1029/2019JD031054

Peterson, M., Mach, D., & Buechler, D. (2021). A Global LIS/OTD Climatology of Lightning Flash Extent Density. *Journal of Geophysical Research: Atmospheres*, *126*(8), e2020JD033885. https://doi.org/10.1029/2020JD033885

Peterson, M., Rudlosky, S., & Zhang, D. (2020). Thunderstorm Cloud-Type Classification from Space-Based Lightning Imagers. *Monthly Weather Review*, *148*(5), 1891–1898. https://doi.org/10.1175/MWR-D-19-0365.1

Peterson, M., & Stano, G. (2021). The Hazards Posed by Mesoscale Lightning Megaflashes. *Earth Interactions, 25*(1), 46–56. https://doi.org/10.1175/EI-D-20-0016.1

Plant Bowen Info Sheet. (2016). Georgia Power. https://www.georgiapower.com/content/dam/georgia-power/pdfs/company-pdfs/plant-bowen/2016-plant-bowen-info-sheet.pdf

Rakov, V. A., & Uman, M. A. (2006). *Lightning: Physics and Effects*. Cambridge University Press.

Raman, S., Sims, A., Ellis, R., & Boyles, R. (2005). Numerical Simulation of Mesoscale Circulations in a Region of Contrasting Soil Types. *Pure and Applied Geophysics*, *162*(8), 1689–1714. https://doi.org/10.1007/s00024-005-2689-4

Ringhausen, J., Bitzer, P., Koshak, W., & Mecikalski, J. (2021). Classification of GLM Flashes Using Random Forests. *Earth and Space Science*, *8*(11), e2021EA001861. https://doi.org/10.1029/2021EA001861

Romps, D. M., Seeley, J. T., Vollaro, D., & Molinari, J. (2014). Projected increase in lightning strikes in the United States due to global warming. *Science*, *346*(6211), 851–854. https://doi.org/10.1126/science.1259100

Rose, L., Stallins, J., & Bentley, M. (2008). Concurrent Cloud-to-Ground Lightning and Precipitation Enhancement in the Atlanta, Georgia (United States), Urban Region. *Earth Interactions - EARTH INTERACT, 12*, 1–30. https://doi.org/10.1175/2008EI265.1

Rosenfeld, D., Lohmann, U., Raga, G., O'Dowd, C., Kulmala, M., Sandro, F., Reissell, A., & Andreae, M. (2008). Flood or drought: How do aerosols affect precipitation? *Science, v.321, 1309-1313 (2008), 321*.

Roubeyrie, L., & Celles, S. (2018). Windrose: A Python Matplotlib, Numpy library to manage wind and pollution data, draw windrose. *Journal of Open Source Software*, *3*(29), 268. https://doi.org/10.21105/joss.00268

Rozoff, C. M., Cotton, W. R., & Adegoke, J. O. (2003). Simulation of St. Louis, Missouri, Land Use Impacts on Thunderstorms. *Journal of Applied Meteorology and Climatology*, *42*(6), 716–738. https://doi.org/10.1175/1520-0450(2003)042<0716:SOSLML>2.0.CO;2

Rudlosky, S. (2020). *Geostationary Lightning Mapper Value Assessment*. https://doi.org/10.25923/2616-3V73

Rudlosky, S. D., Goodman, S. J., Virts, K. S., & Bruning, E. C. (2019). Initial Geostationary Lightning Mapper Observations. *Geophysical Research Letters*, *46*(2), 1097–1104. https://doi.org/10.1029/2018GL081052

Schmid, P. E., & Niyogi, D. (2013). Impact of city size on precipitation-modifying potential. *Geophysical Research Letters*, *40*(19), 5263–5267. https://doi.org/10.1002/grl.50656

Schultz, C. J., Andrews, V. P., Genareau, K. D., & Naeger, A. R. (2020). Observations of lightning in relation to transitions in volcanic activity during the 3 June 2018 Fuego Eruption. *Scientific Reports*, *10*(1), 18015. https://doi.org/10.1038/s41598-020-74576-x

Schultz, C. J., Petersen, W. A., & Carey, L. D. (2011). Lightning and Severe Weather: A Comparison between Total and Cloud-to-Ground Lightning Trends. *Weather and Forecasting*, *26*(5), 744–755. https://doi.org/10.1175/WAF-D-10-05026.1

Schultz, M. D., Underwood, S. J., & Radhakrishnan, P. (2005). A Method to Identify the Optimal Areal Unit for NLDN Cloud-to-Ground Lightning Flash Data Analysis. *Journal of Applied Meteorology and Climatology*, *44*(5), 739–744. https://doi.org/10.1175/JAM2234.1

Schulzweida, U. (2022). *CDO User Guide (2.1.0)*. Zenodo. https://doi.org/10.5281/zenodo.7112925

Shamsipour, A., Azizi, G., Karimi, M., & Moghbel, M. (2013). Surface temperature pattern of asphalt, soil and grass in different weather condition. *Journal of BIodIversIty and EnvIronmental ScIences*, *3*, 80–89.

Shem, W., & Shepherd, M. (2009). On the impact of urbanization on summertime thunderstorms in Atlanta: Two numerical model case studies. *Atmospheric Research*, *92*(2), 172–189. https://doi.org/10.1016/j.atmosres.2008.09.013

Shepherd, J. M. (2005). A Review of Current Investigations of Urban-Induced Rainfall and Recommendations for the Future. *Earth Interactions*, *9*(12), 1–27. https://doi.org/10.1175/EI156.1

Shepherd, J. M., Pierce, H., & Negri, A. J. (2002). Rainfall Modification by Major Urban Areas: Observations from Spaceborne Rain Radar on the TRMM Satellite. *Journal of Applied Meteorology and Climatology*, *41*(7), 689–701. https://doi.org/10.1175/1520-0450(2002)041<0689:RMBMUA>2.0.CO;2

Shepherd, M., Andersen, T., Strother, C., Horst, A., Bounoua, L., & Mitra, C. (2014). Urban Climate Archipelagos: A new Framework for urban impacts on climate. *Earthzine*.

Shepherd, M., Mote, T., Mccutcheon, S., Knox, P., Dowd, J., & Roden, M. (2011). Unique perspectives on how synoptic forcing and urban land cover contributed to the disastrous Atlanta flood of 2009. *Bulletin of the American Meteorological Society*, *92*, 861–870.

Shepherd, M., Stallins, J., Jin, M. L., & Mote, T. (2015). *Urbanization: Impacts on Clouds, Precipitation, and Lightning* (pp. 1–28). https://doi.org/10.2134/agronmonogr55.c1

Simpson, M. (2006). *Role of urban land use on mesoscale circulations and precipitation*.

Sims, A. P., & Raman, S. (2016). Interaction Between Two Distinct Mesoscale Circulations During Summer in the Coastal Region of Eastern USA. *Boundary-Layer Meteorology*, *160*(1), 113–132. https://doi.org/10.1007/s10546-015-0125-6

Snyder, J. P. (1987). *Map projections: A working manual*. USGS. https://doi.org/10.3133/pp1395

Sokol, N. J., & Rohli, R. V. (2018). Land cover, lightning frequency, and turbulent fluxes over Southern Louisiana. *Applied Geography*, *90*, 1–8. https://doi.org/10.1016/j.apgeog.2017.11.003

Srivanit, M., & Hokao, K. (2012). Thermal Infrared Remote Sensing for Urban Climate and Environmental Studies: An Application for the City of Bangkok, Thailand. *Journal of Architectural/Planning Research and Studies (JARS)*, *9*, 83–100.

Stallins, J. (2004). Characteristics of Urban Lightning Hazards for Atlanta, Georgia. *Climatic Change*, *66*, 137–150. https://doi.org/10.1023/B:CLIM.0000043135.13801.71

Stallins, J., & Bentley, M. (2006). Urban lightning climatology and GIS: An analytical framework from the case study of Atlanta, Georgia. *Applied Geography, 26*, 242–259. https://doi.org/10.1016/j.apgeog.2006.09.008

Stallins, J., Bentley, M., & Rose, L. (2006). Cloud-to-ground flash patterns for Atlanta, Georgia (USA) from 1992 to 2003. *Climate Research - CLIMATE RES*, *30*, 99–112. https://doi.org/10.3354/cr030099

Stallins, J., Carpenter, J., Bentley, M., Ashley, W., & Mulholland, J. (2012). Weekend–weekday aerosols and geographic variability in cloud-to-ground lightning for the urban region of Atlanta, Georgia, USA. *Regional Environmental Change*, *13*. https://doi.org/10.1007/s10113-012-0327-0

Stallins, J., & Rose, L. (2008). Urban Lightning: Current Research, Methods, and the Geographical Perspective. *Geography Compass*, *2*, 620–639. https://doi.org/10.1111/j.1749-8198.2008.00110.x

Stano, G. T., Smith, M. R., & Schultz, C. J. (2019). Development and Evaluation of the GLM Stoplight Product for Lightning Safety. *Journal of Operational Meteorology*, 92–104. https://doi.org/10.15191/nwajom.2019.0707

Steiger, S. M., & Orville, R. E. (2003). Cloud-to-ground lightning enhancement over Southern Louisiana. *Geophysical Research Letters*, *30*(19). https://doi.org/10.1029/2003GL017923

Steiger, S. M., Orville, R. E., & Huffines, G. (2002). Cloud-to-ground lightning characteristics over Houston, Texas: 1989–2000. *Journal of Geophysical Research: Atmospheres*, *107*(D11), ACL 2-1-ACL 2-12. https://doi.org/10.1029/2001JD001142

Strikas, O. M., & Elsner, J. B. (2013). Enhanced cloud-to-ground lightning frequency in the vicinity of coal plants and highways in Northern Georgia, USA. *Atmospheric Science Letters*, *14*(4), 243–248. https://doi.org/10.1002/asl2.446

Student. (1908). The Probable Error of a Mean. *Biometrika*, *6*(1), 1–25. https://doi.org/10.2307/2331554

Teller, A., & Levin, Z. (2008). Factorial method as a tool for estimating the relative contribution to precipitation of cloud microphysical processes and environmental conditions: Method and application. *Journal of Geophysical Research*, *113*. https://doi.org/10.1029/2007JD008960

Terando, A. J., Costanza, J., Belyea, C., Dunn, R. R., McKerrow, A., & Collazo, J. A. (2014). The Southern Megalopolis: Using the Past to Predict the Future of Urban Sprawl in the Southeast U.S. *PLoS ONE*, *9*(7), e102261. https://doi.org/10.1371/journal.pone.0102261

Tilles, J. N., Liu, N., Stanley, M. A., Krehbiel, P. R., Rison, W., Stock, M. G., Dwyer, J. R., Brown, R., & Wilson, J. (2019). Fast negative breakdown in thunderstorms. *Nature Communications*, *10*(1), Article 1. https://doi.org/10.1038/s41467-019-09621-z

Tinmaker, M. I. R., Jena, C. K., Ghude, S. D., Dwivedi, A. K., Islam, S., Kulkarni, S. H., Khare, M. K., & Chate, D. M. (2021). Relationship of lightning with different weather parameters during transition period of dry to wet season over Indian region. *Journal of Atmospheric and Solar-Terrestrial Physics*, *220*, 105673. https://doi.org/10.1016/j.jastp.2021.105673

Tukey, J. W. (1949). Comparing Individual Means in the Analysis of Variance. *Biometrics*, *5*(2), 99–114. https://doi.org/10.2307/3001913

Uman, M. A. (2001). *The Lightning Discharge*. Courier Corporation.

Wang, H., Shi, Z., Wang, X., Tan, Y., Wang, H., Li, L., & Lin, X. (2021). Cloud-to-Ground Lightning Response to Aerosol over Air-Polluted Urban Areas in China. *Remote Sensing*, *13*(13), Article 13. https://doi.org/10.3390/rs13132600

Watson, A. I., & Holle, R. L. (1996). An Eight-Year Lightning Climatology of the Southeast United States Prepared for the 1996 Summer Olympics. *Bulletin of the American Meteorological Society*, *77*(5), 883–890. https://doi.org/10.1175/1520-0477(1996)077<0883:AEYLCO>2.0.CO;2

Westcott, N. E. (1995). Summertime Cloud-to-Ground Lightning Activity around Major Midwestern Urban Areas. *Journal of Applied Meteorology and Climatology*, *34*(7), 1633–1642. https://doi.org/10.1175/1520-0450-34.7.1633

Wootten, A., Raman, S., & Sims, A. (2010). Diurnal variation of precipitation over the Carolina Sandhills region. *Journal of Earth System Science*, *119*(5), 579–596. https://doi.org/10.1007/s12040-010-0045-2

Yair, Y. (2018). Lightning hazards to human societies in a changing climate. *Environmental Research Letters*, *13*(12), 123002. https://doi.org/10.1088/1748-9326/aaea86

Yang, L., Jin, S., Danielson, P., Homer, C., Gass, L., Bender, S. M., Case, A., Costello, C., Dewitz, J., Fry, J., Funk, M., Granneman, B., Liknes, G. C., Rigge, M., & Xian, G. (2018). A new generation of the United States National Land Cover Database: Requirements, research priorities, design, and implementation strategies. *ISPRS Journal of Photogrammetry and Remote Sensing*, *146*, 108–123. https://doi.org/10.1016/j.isprsjprs.2018.09.006

Zender, C. S. (2022). *NetCDF Operator User Guide*. http://nco.sf.net/nco.pdf

Zhang, D., & Cummins, K. L. (2020). Time Evolution of Satellite-Based Optical Properties in Lightning Flashes, and its Impact on GLM Flash Detection. *Journal of Geophysical Research: Atmospheres*, *125*(6), e2019JD032024. https://doi.org/10.1029/2019JD032024

Zhang, X., Yin, Y., Kukulies, J., Li, Y., Kuang, X., He, C., Lapierre, J. L., Jiang, D., & Chen, J. (2021). Revisiting Lightning Activity and Parameterization Using Geostationary Satellite Observations. *Remote Sensing*, *13*(19), Article 19. https://doi.org/10.3390/rs13193866

Zhao, P., Li, Z., Xiao, H., Wu, F., Zheng, Y., Cribb, M. C., Jin, X., & Zhou, Y. (2020). Distinct aerosol effects on cloud-to-ground lightning in the plateau and basin regions of Sichuan, Southwest China. *Atmospheric Chemistry and Physics*, *20*(21), 13379–13397. https://doi.org/10.5194/acp-20-13379-2020

Zhao, P., Zhou, Y., Xiao, H., Liu, J., Gao, J., & Ge, F. (2017). Total Lightning Flash Activity Response to Aerosol over China Area. *Atmosphere*, *8*(2), Article 2. https://doi.org/10.3390/atmos8020026